ARCHIVES OF MECHANICS
Arch. Mech. **73** (5–6), 599–633, 2021, DOI: 10.24423/aom.3857

Magnetohydrodynamic effect on axisymmetric Stokes flow past a weakly permeable spheroid with a solid core

M. K. PRASAD, T. BUCHA

Department of Mathematics, National Institute of Technology, Raipur-492010, Chhattisgarh, India,
e-mails: madaspramaths@nitrr.ac.in, kpm973@gmail.com, tinabucha11@gmail.com

The current research is focused on the creeping motion of fluid past a permeable spheroidal particle that has an impermeable core under the magnetic forces. Motion in the permeable zone is proposed to be regulated by Darcy's law. At the fluid-porous interface, the continuity of the normal velocity component is assumed together with the balance of pressure with normal stresses and the Beavers–Joseph–Saffman–Jones (BJSJ) slip boundary condition. Vanishing of the normal component of velocity is used at the surface of the impermeable core. The drag on the spheroidal particle is obtained in an analytical form. The reliability of the drag coefficient on significant physical parameters such as permeability, non-sphericity parameter, Hartmann numbers, separation parameter (the measure of closeness between the porous particle and the core), and slip parameters is examined. Comparisons of results are made with the cases having no magnetic effect and show that the applied magnetic field possesses the ability to reduce the rate of flow of fluid. Well-known previously published results are deduced from the current analysis.

Key words: spheroid, MHD effect, modified Stokes law, modified Darcy's law, BJSJ condition, drag.

1. Introduction

In the vast expansion and scope of fluid mechanics, the interest in exploring the class of flows past porous bodies of various shapes is explained through their applications in science and engineering. In the applications of such flows, it is most important to know the technique for controlling the condition of the physical problem under inspection. To control the rate of flow of fluid, researchers are keenly focusing on the transport properties of fluids. One among them is the study of the flow of fluid in the existence of applied magnetic forces known as magnetohydrodynamic flow (MHD). MHD studies the relation between the magnetic fields and the fluid in motion. The subject evolved rapidly and turned out to be an important area of conversation for the scientific and academic community. Also, a resisting force, popularly recognized as the the Lorentz force comes into play when dealing with the MHD flow. This force acts in a direction

reverse to the flow generated by the magnetic field [1] as per Lenz's law (which says the current that is induced in a circuit because of the change in the magnetic field is aimed to restrict the alteration in flux and to apply a mechanical force that restricts the movement) and reduces the velocity of the fluid flow [2].

In the last few decades, classes of problems dealing with flow past porous media are treated with the utmost care, as such flows can be easily found in nature and man-made flows like flow through packed beds, oil movement within porous rocks, porous pellets used in catalytic reactions, sedimentation of particles, solid-fluid filtration, drug diffusion past human skin, etc. Also, a more precious kind of membrane having very low permeability that only permits the specific type of particles to flow is known as a semipermeable membrane. For example, one can find its application in the process of osmosis, a process that is diffusive in nature. Applying magnetic effects in such flows seems to have an impact on the pattern of the flow. Many investigators worked tremendously on the problems concerning flow past porous bodies. Focusing on the discrepancies while formulating flow past porous particles in terms of choosing transport governing equations, we come across an empirical relation proposed by Darcy [3]. Darcy's law assumes the component of velocity to be proportional directly to the pressure gradient where no convective term exists. Hence, this law is well applicable to modeling problems bearing low permeability. On the contrary, Brinkman's equation [4], which is a generalized Darcy's law, is used for describing problems with a large shear rate and higher porosity. While dealing with the flow past porous bodies an interface appears separating the porous body from the pure fluid. Owing to the study of low permeability problems, a matter of major concern is choosing the proper boundary conditions. The standard no-slip condition was frequently applied at the interface. Later, it was claimed that this condition may not always be useful to completely describe the real phenomena and thus the conditions including slip effect were put forward by Beavers and Joseph [5], Saffman [6].

Numerous early works dealing with the porous flow shed light on the variation of the flow pattern for varying particle geometry [7–12]. Apart from the above articles, Jacob *et al.* [13] investigated the slow flow through a sphere bearing a rigid core with a porous shell. Raja Sekhar and Amarnath [14] investigated the movement of fluid through a porous sphere containing a solid core by using Darcy's law. Feng and Michaelides [15] examined the finite but low Reynolds number flow past a permeable particle of the spherical structure. Additionally, Jager and Mikelic [16] made a study to explore the boundary conditions put forward by Beavers, Joseph, and Saffman. Previously, Vainshtein *et al.* [17] inspected the creeping flow through and inside a permeable spheroidal particle. An analysis of the Stokes flow around a porous sphere with an impervious core by employing the stress jump condition has been carried out by Bhattacharyya and Raja Sekhar [18]. Senchenko and Keh [19] scrutinized the flow past

a slightly distorted sphere. SRIVASTAVA and SRIVASTAVA [20] analyzed the fluid flow past a porous sphere together with an impermeable spherical core by considering Brinkman's equation. SRINIVASACHARYA [21] talked about the slow flow through a porous shell of approximately spherical geometry, which was proposed to be studied by Darcy's law. In their work, they took into consideration the following boundary conditions: continuity of normal velocity, Beavers–Joseph slip condition and the continuity of pressure. URQUIZA *et al.* [22] reported the coupling of the Stokes–Darcy equation while studying the motion in porous media, where they considered Beavers–Joseph–Saffman conditions. SHAPOVALOV [23] treated the flow past a semipermeable spherical particle through an analytical approach and made the use of the boundary conditions as mentioned in [8]. A semipermeable particle is a particle bearing very low permeability such that the velocity's tangential component can be considered zero at the interface. The result shows that the drag force on the semipermeable particle is lower as compared to the drag on a non-permeable particle. Furthermore, CAO *et al.* [24] talked about the Coupled Stokes–Darcy model considering Beavers–Joseph slip condition. SAAD [25] analyzed the translational as well as the rotational motion of the porous spheroid inside a cell and obtained the drag and the couple experienced on a prolate and an oblate spheroidal cases. VERESHCHAGIN and DOLGUSHEV [26] tackled the motion of incompressible viscous fluid bearing very low velocity through a hollow porous sphere, using the slip (Beavers–Joseph) and the no-slip conditions at the interface. PRAKASH *et al.* [27] studied the Stokes flow past a porous particle by choosing both Brinkman's and Darcy's law, separately. Under these circumstances, the overall bed (a collection of uniform porous spheres) permeability has been compared for both cases. YADAV and DEO [28] made an analysis of the viscous flow past a deformed porous sphere inside a different porous medium. In an article by SAAD [29], the investigation of the Stokes flow past a porous spheroid inside a spheroidal vessel was reported. Flow through a porous approximate sphere (particle shape deviates from the spherical shape) bearing an impermeable core both in the bounded and unbounded domains have been handled by SRINIVASACHARYA and PRASAD [30, 31]. The motion of fluid in the porous media is considered to be ruled by Brinkman's equation. They obtained the expressions of the drag on the porous approximate spherical particle. Moreover, SRINIVASACHARYA and PRASAD [32] analyzed the flow past a body of approximately spherical shape inside an approximately spherical container. SHERIEF *et al.* [33] have analyzed the problem concerned about the oscillation of spheroidal particle inside a micropolar fluid and have paid attention to the slip on the particle surface. PRAKASH and RAJA SHEKAR [34] determined the dynamic permeability for the assemblage of spherical permeable particles by taking into account the Saffman boundary condition. The bed permeability for the steady flow is known as the hydrodynamic permeability and for the oscillatory

motion is the dynamic permeability, which for the latter condition relies on the frequency parameter and may be a complex valued function. Yadav *et al.* [35] investigated the slow motion of fluid through a swarm of porous spheroidal particles by using the concept of particle in cell. The drag force and the membrane permeability of porous spheroids are calculated and their dependence on various flow parameters are calculated. Extracting fluid via porous media through a slender permeable prolate-spheroidal structure was handled by Chen [36]. Applying Beavers–Joseph–Saffman's condition, Rasoulzadeh and Kuchuk [37] focused on finding the effective permeability of a spherical and a spheroidal cavity of the porous medium that contains fracture inclusion. Also, Tiwari *et al.* [38] handled the problem of in-homogeneous porous cylindrical particles by considering Darcy's law along with using the Beavers–Joseph slip interface condition. Besides, Prasad and Kaur [39], in their work of flow past a spheroidal droplet containing micropolar fluid demonstrated the reliability of the wall correction factor on several flow parameters. Yadav *et al.* [40] studied the motion of an incompressible flow through a membrane of spheroidal particles with a porous layer. Considering the Saffman's boundary condition, Khabthani *et al.* [41] examined the lubricating motion of a sphere nearing a porous thin slab. Moreover, Ming *et al.* [42] made a study on the simple projection technique for understanding the coupling of Navier–Stokes and Darcy flows by implementing the Beavers–Joseph–Saffman condition. Employing the Beavers–Joseph–Saffman–Jones condition, Prasad and Bucha [43] analyzed the motion of a permeable spheroid and evaluated an exact expression for the drag force exerted on it. Recently, Prasad [44] has studied the boundary effects on an eccentric semipermeable sphere by considering the cell model technique. Cell models are one of the most regularly used models for reporting the interactions of particles regarding proper boundary conditions where any typical particle is covered through a hypothetical liquid envelope by which the hydrodynamic interactions are controlled.

The era of modern science is concerned with studying the MHD principle to explore the coupling between the magnetic field and fluid flow, as it enjoys a wider domain of applications in the varying fields of science. Application of such MHD is also observed in the delivery of drugs to the required area, medical cure of tumors, cancer, and many more. In the books by Cramer and Pai [45], Davidson [46], a basic review of MHD flow can be well studied. Various brilliant works contributed by numerous researchers emphasize the important aspects of this rapidly growing field [47–51]. Later, Geindreau and Aurialt [52] have carried the study of the filtration flow through a rigid Darcy's porous media by taking into account the MHD effect. From their work, it was observed that the permeability tensor greatly relies on the Hartmann number and is symmetric and positive definite. Furthermore, several other problems dealing with the magnetic effect have been considered by Verma and Datta [53], Jayalak-

SHMAMMA *et al.* [54], SRIVASTAVA and DEO [55]. To assess the impact of the external magnetic field, SRIVASTAVA *et al.* [56] examined the hydrodynamic permeability of a membrane containing porous particles of spherical shape. VERMA and SINGH [57] analyzed the problem of a circular channel packed with a porous medium. Intending to find the effect of magnetic forces, YADAV *et al.* [58] studied the hydrodynamic permeability of a membrane composed of spherical particles having a porous shell. As per one of the recent studies done by SAAD [59], the impact of the magnetic forces on the flow through a porous sphere and cylinder surrounded by a cell has a dominating effect on the flow pattern. Thereafter, PRASAD and BUCHA [60] investigated the MHD influence on the motion of the fluid past a semipermeable spherical particle and founded an expression for drag. Subsequently, PRASAD and BUCHA [61] carried out an analytical investigation of parallel MHD flow past a cylindrical shell in which the porous region is ruled by Brinkman's model. In this evaluation, they observed the substantial effect of applying the magnetic field on the nature of the flow. In a recent article by PRASAD and BUCHA [62], the presence of magnetic forces has been seen to affect the creeping flow of fluid sphere (sphere filled with fluid) and bounded by a spherical envelope. YADAV [63] has investigated the impact of magnetic field on movement past a porous spheroid in a cell by using the perturbation method and has further analyzed the hydrodynamic permeability of the membrane. Hydrodynamic permeability acting on the weakly permeable sphere and cylinder, due to the creeping flow of viscous fluid under the magnetic field was mentioned in the articles by PRASAD and BUCHA [64, 65]. Recently, PRASAD and BUCHA [66] have demonstrated the influence of magnetic forces on the flow of a porous spheroid governed by Brinkman's model and further evaluated the drag acting on it. As the MHD effects are varying with particle geometry, it is of much importance to explore magnetic fields effect for different configurations of particles. BUCHA and PRASAD [67] presented the viscous flow of fluid through a low permeable spheroid in a spheroidal cell. PRASAD *et al.* [68] gave emphasis on the Stokes flow past a solid spheroid which is imposed in Brinkman's porous media.

Currently, we extend the analysis made by PRASAD and BUCHA [43] for the fluid motion past a permeable spheroidal particle with an impermeable core in the presence of the applied magnetic field. Applications of the current study can be found in energy extraction from geothermal zones, in combustion in an inert porous matrices, in the underground spreading of chemical waste, chemical catalytic reactors. In the dispersion of cholesterol and other fatty compounds from human arteries to endothelium, modeling of polymer macromolecule coils in a solvent. Porous particles in a variety of geometrical shapes, which differ significantly from spheres. To understand this concept of practical application, one must first comprehend how fluid flows past/through a body. And these practical issues necessitate a system to control the movement of fluid past solid bodies

with MHD effects [18]. This interdisciplinary topic has gotten a lot of interest recently because of its wide variety of applications in science and industry. Fluid and thermal sciences, geothermal, petroleum, and combustion engineering are all part of the study of porous media in a wide sense. In chemical engineering, especially in industry, the word that is often used is chemical agglomeration. The enlargement of solid particles is called agglomeration. A common method of agglomeration technique involves partial melting, absorption of moisture from the air, electrostatic adhesion and pressing. Tablets, fertiliser pellets, fly ash, and charcoal briquettes are just a few examples of products that require agglomeration to form the final product. The submergence of permeable agglomerates in their treatment means determines their progressive infiltration by the liquid. In modern metallurgical and metal working operations, the study of MHD flows of electrically conducting fluids in electric and magnetic fields is very appealing. This has sparked a lot of interest in the study of boundary layer flows subjected to external magnetic fields.

This specific problem is chosen as it involves two separate interfaces of interest: a porous-clear fluid interface on the spheroid's outer surface, and a porous-impermeable interface at the core boundary. Also, it is of considerable importance in the amending of rigid particles in a chemical reactor including different catalytic solid-gas reaction: specifically sulphuring of dolomite or limestone, and combustion of oil shale [31]. The further flow through porous particles has plenty of commercial uses including a filtration procedure, in a broad range for separating solute from the solvent, in the desalination process for brackish seawater, and in purifying water, juice, sugars, in treating wastewater, etc. The elimination of particles and the adherence of chemical species to the surfaces of solid particles occur during filtration. This procedure results in the emergence of a porous layer on the solid particles and it directly affects the hydrodynamic drag experienced by the particles [69]. The current study aims to analyze such flows. In the work under consideration, the model of fluid flow past a permeable spheroid with an impenetrable core in presence of magnetic forces is examined. An analytical solution for the drag exercised on such particles has been evaluated. The influence of several non-dimensional parameters that emerged during the study including permeability, slip, non-sphericity parameter, the Hartmann number, and separation parameters on the behaviour of the coefficient of drag is examined.

2. Problem formulation

Proposed mathematical model

The magnetic effect on the slow, steady, and axisymmetric movement of conducting fluid past a permeable spheroidal particle of radius $r_a \equiv r = a[1+2\epsilon\vartheta_2(\zeta)]$ with a rigid core of radius $r_b \equiv r = b[1+2\epsilon\vartheta_2(\zeta)]$ is considered where ϵ and $\vartheta_2(\zeta)$

are the non-sphericity parameter and the Gegenbauer function with $\zeta = \cos\theta$, and a & b are the radius of the permeable spherical particle and spherical core, respectively (see Fig. 1). The uniform magnetic field is enforced in the flow's transverse direction, and the permeable particle move with uniform velocity U in the z direction. The magnetic Reynolds number, represented as $Re_m = Ua\mu_h\sigma$ is assumed to be immensely small in which σ represents fluids electrical conductivity and μ_h the magnetic permeability. Further μ_h is assumed to be the same for the fluid as well as a porous region. Any applied external electric field is absent, and the presence of the induced magnetic field is ignored because the magnetic Reynolds number is considered to be small enough.

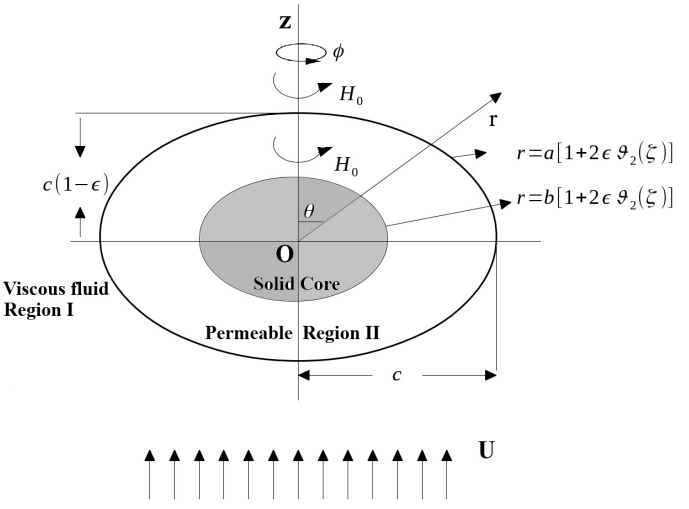

FIG. 1. Schematic draft of flow past a permeable oblate spheroid with core with non-sphericity parameter ϵ, $\vartheta_2(\zeta)$ the Gegenbauer function and $\zeta = \cos\theta$.

Spherical polar coordinates (r, θ, ϕ) together with $(\mathbf{e}_r, \mathbf{e}_\theta, \mathbf{e}_\phi)$ as unit base vectors are implemented for solving the problem. The viscous fluid region I and permeable region II are represented by i, in which $i = 1, 2$, respectively.
The flow is axially symmetric, indicating the independence of all the flow quantities on ϕ. We employ velocity vectors as

$$\mathbf{v}^{(i)} = v_r^{(i)}(r,\theta)\mathbf{e}_r + v_\theta^{(i)}(r,\theta)\mathbf{e}_\theta, \quad i = 1, 2. \tag{2.1}$$

The modified Maxwell equations [2, 45] governing MHD flow are

$$\nabla \times \mathbf{H} = \mu_h \mathbf{J}, \tag{2.2}$$

$$\nabla \cdot \mathbf{J} = 0, \tag{2.3}$$

$$\nabla \times \mathbf{E} = -\frac{\partial H}{\partial t}, \tag{2.4}$$

$$\nabla \cdot \mathbf{H} = 0. \tag{2.5}$$

Also,

$$\mathbf{J} = \mu_h \sigma \left(\mathbf{E} + \mathbf{v} \times \mathbf{H}\right), \tag{2.6}$$

where $\mathbf{J}$, $\mathbf{H}$, $\mathbf{E}$, are the electric current density, magnetic field intensity, and the electric field, respectively.

As the current (density J) is flowing across the field, $\mathbf{H}$ implies that the Lorentz force $\mathbf{F}$ (in case of conducting fluid) per unit volume acts on a spheroid [2, 70, 71] and is given as

$$\mathbf{F} = \mu_h \mathbf{J} \times \mathbf{H}. \tag{2.7}$$

Now, using Eqs. (2.6) and (2.7), we have

$$\mathbf{F} = \mu_h^2 \sigma (\mathbf{E} + \mathbf{v} \times \mathbf{H}) \times \mathbf{H}. \tag{2.8}$$

Moreover, the presence of any external electric field is ignored i.e., $E = 0$. Thus,

$$\mathbf{F} = \mu_h^2 \sigma \left(\mathbf{v} \times \mathbf{H}\right) \times \mathbf{H}, \tag{2.9}$$

where $\mathbf{v}$ is the velocity of the fluid.

The magnetic force present in the fluid momentum equation modifies the pressure and viscous stress with respect to the problem in absence of a magnetic field. Here, the modified Stokes equation is a combination of Stokes equation with the Lorentz force term, and modified Darcy's equation is a combination of Darcy's law with the Lorentz force term. Therefore, the modified Stokes equation [59, 60, 62, 72] regulates the flow in region I and the modified Darcy equation [3, 52, 60, 64, 65] regulates the flow in region II. Also, the magnetic field is considered to be in a transverse direction, therefore $\mathbf{H}^{(i)} = H_o \mathbf{e}_\phi$, $i = 1, 2$.

Flow governing equations

The equations that regulates the motion in region I are given by modified Stokes equation as

$$\nabla \cdot \mathbf{v}^{(1)} = 0, \tag{2.10}$$

$$\nabla p^{(1)} + \mu \nabla \times \nabla \times \mathbf{v}^{(1)} - \mu_h^2 \sigma (\mathbf{v}^{(1)} \times \mathbf{H}^{(1)}) \times \mathbf{H}^{(1)} = 0. \tag{2.11}$$

Equations for the movement of fluid in permeable region II regulated by modified Darcy's law as

$$\nabla \cdot \mathbf{v}^{(2)} = 0, \tag{2.12}$$

$$\nabla p^{(2)} + \frac{\mu}{k} \mathbf{v}^{(2)} - \mu_h^2 \sigma (\mathbf{v}^{(2)} \times \mathbf{H}^{(2)}) \times \mathbf{H}^{(2)} = 0, \tag{2.13}$$

where $\mathbf{v}^{(i)}$, $p^{(i)}$, μ, σ are velocity, pressure, coefficient of viscosity, fluids electric conductivity, and k the permeability of porous region.

The below mentioned dimensionless variables are applied to transform the flow governing equations into non-dimensional form,

$$r = a\tilde{r}, \quad \nabla = \frac{\tilde{\nabla}}{a}, \mathbf{v}^{(i)} = U\tilde{\mathbf{v}}^{(i)}, \quad p^{(i)} = \frac{\mu U}{a}\tilde{p}^{(i)}, \quad \mathbf{H}^{(i)} = H_o \quad \tilde{\mathbf{H}}^{(i)}. \tag{2.14}$$

After placing the above substitution in Eqs. (2.10) to (2.13) and skipping the tildes, the final equations are written as

$$\nabla \cdot \mathbf{v}^{(1)} = 0, \tag{2.15}$$

$$\nabla p^{(1)} + \nabla \times \nabla \times \mathbf{v}^{(1)} - \alpha^2(\mathbf{v}^{(1)} \times \mathbf{H}^{(1)}) \times \mathbf{H}^{(1)} = 0, \tag{2.16}$$

$$\nabla \cdot \mathbf{v}^{(2)} = 0, \tag{2.17}$$

$$\nabla p^{(2)} + \xi^2 \mathbf{v}^{(2)} - \chi^2(\mathbf{v}^{(2)} \times \mathbf{H}^{(2)}) \times \mathbf{H}^{(2)} = 0, \tag{2.18}$$

where

- $\alpha = \sqrt{\dfrac{\mu_h^2 H_o^2 \sigma a^2}{\mu}}$, the Hartmann number for liquid region I.
- $\chi = \sqrt{\dfrac{\mu_h^2 H_o^2 \sigma a^2}{\varepsilon\mu}}$, the Hartmann number for permeable region II with ε to be the porosity [59].
- $\xi^2 = \dfrac{a^2}{k}$, the dimensionless permeability parameters.
- Also, we represent $\beta^2 = \xi^2 + \chi^2$.

The spheroidal surface should have the shape of $r = a\,[1 + f(\theta)]$ [72]. It has a slightly different shape from the spherical surface $r = a$. Normally, the orthogonality relationships of Gegenbauer functions $\vartheta_m(\zeta)$, $\zeta = \cos\theta$ allow us to investigate the expansion $f(\theta) = \sum_{k=2}^{\infty} \alpha_k \vartheta_k(\zeta)$ [29, 43, 66, 74].

In the equation above, the Gegenbauer function in respect to the Legendre function $P_n(\zeta)$ is represented as

$$\vartheta_n(\zeta) = \frac{P_{n-2}(\zeta) - P_n(\zeta)}{2n-1}, \quad n \geq 2. \tag{2.19}$$

Thus, the spheroidal surface can be picked as

$$r = a[1 + \alpha_m \vartheta_m(\zeta)] \equiv r_a \tag{2.20}$$

and the radius of the deformed core as

$$r = b[1 + \alpha_m \vartheta_m(\zeta)] \equiv r_b \tag{2.21}$$

along with the coefficient α_m predicted to be sufficiently small so that squares and higher powers of α_m's are ignored, i.e., neglecting the terms of $O(\alpha_m^2)$ [72, 74]. Further, $(r/a)^l \approx 1 + l\alpha_m \vartheta_m(\zeta)$ in which l is either positive or negative.

The solution for $r = a[1 + \sum_m \alpha_m \vartheta_m(\zeta)]$ can be constructed from the result of (2.20) and (2.21).

Let $\psi^{(i)}$ be the stream functions for liquid and permeable regions, respectively with $i = 1, 2$.

The stream functions in correspondence to the velocity components are

$$v_r^{(i)} = \frac{1}{r^2}\frac{\partial \psi^{(i)}}{\partial \zeta}, \quad v_\theta^{(i)} = \frac{1}{r\sqrt{1-\zeta^2}}\frac{\partial \psi^{(i)}}{\partial r}, \quad i = 1, 2. \tag{2.22}$$

The removal of the pressure terms $p^{(1)}$ and $p^{(2)}$ from Eqs. (2.16) and (2.18), produces

$$E^2(E^2 - \alpha^2)\psi^{(1)} = 0, \tag{2.23}$$

$$E^2\psi^{(2)} = 0, \tag{2.24}$$

in which, $E^2 = \dfrac{\partial^2}{\partial r^2} + \dfrac{1-\zeta^2}{r^2}\dfrac{\partial^2}{\partial \zeta^2}$ is the Stokes operator.

3. Boundary conditions

The need to evaluate the flow velocity while studying flow through the permeable spheroidal particle requires proper boundary conditions that support the physics and mathematics of the problem. While studying the flow regulated by Darcy's law, the frequently used condition of pressure continuity $p^{(1)} = p^{(2)}$ is suitable for the flow past a perfect sphere but for the case of a low permeable spheroidal particle this condition seems not to be suitable. Therefore, to consider the effect of deformation the jump condition for pressure $\mathbf{n} \cdot t^{(1)} \cdot \mathbf{n} = -p^{(2)}$ i.e., the normal stress in the fluid area is balanced with the pressure in the permeable area is considered, where $t^{(1)}$ represents the stress tensor for the viscous fluid [37, 43]. The pressure jump condition expresses the balancing of two forces along the normal direction at the interface: the pressure in the porous region and the normal component of the normal stress in the fluid region [37]. Thus, the continuity of normal components of velocities, the proportionality of shear force to the tangential component of the velocity (Beavers–Joseph–Saffman–Jones condition) [5, 6, 11, 37] and a condition for the jump in pressures [37, 38] are found to be more realistic.

On an impermeable core's surface, the vanishing of the normal component of velocity is considered [14]. This is because, in Darcy's equation, the velocity vector field's normal component can only be evaluated on the interface. However, in

the Darcy–Brinkman model, the entire velocity vector field can be defined on the boundary. The mathematical reasoning is that Darcy's equations contain a first-order spatial derivative of the velocity field. Meanwhile, the Darcy-Brinkman model generates a governance equation containing a second-order spatial derivative of the quoted velocity field [75].

Mathematically, at the spheroidal surface $r = a[1 + \alpha_m \vartheta_m(\zeta)]$, we have the following boundary conditions

$$(\mathbf{v}^{(1)} - \mathbf{v}^{(2)}) \cdot \mathbf{n} = 0, \tag{3.1}$$

$$\mathbf{n} \cdot t^{(1)} \cdot \mathbf{s} = \frac{\mu}{\lambda\sqrt{k}} \mathbf{v}^{(1)} \cdot \mathbf{s}, \tag{3.2}$$

$$\mathbf{n} \cdot t^{(1)} \cdot \mathbf{n} = -p^{(2)}, \tag{3.3}$$

at the impermeable core of radius $r = b[1 + \alpha_m \vartheta_m(\zeta)]$,

$$\mathbf{v}^{(2)} \cdot \mathbf{n} = 0. \tag{3.4}$$

In the above equation, λ represents the dimensionless slip coefficient which relies on the character of the porous medium where λ lies in the range of 0.25 and 10 [6, 38, 73]. Precisely, if $\lambda = 0$ and low permeability, the problem resembles the case of flow through a semipermeable spheroidal particle.

Besides, $\mathbf{n}$ is defined in such a way that $\mathbf{n} = \mathbf{e}_r - \alpha_m \sqrt{1-\zeta^2} P_{m-1}(\zeta) \mathbf{e}_\theta$, is the unit normal vector at every point on the spheroidal surface $r = a[1 + \alpha_m \vartheta_m(\zeta)]$ pointing into the fluid [25, 76]. And the normal vector is perpendicular to all the possible surface tangent vectors at that point. Therefore, s is the arbitrary tangential vector introduced as $\mathbf{s} = -\alpha_m \sqrt{1-\zeta^2} P_{m-1}(\zeta) \mathbf{e}_r - \mathbf{e}_\theta$.

The boundary condition at infinity ($r \to \infty$) for the external stream are written as

$$v_r^{(1)} = -U \cos\theta \quad \text{and} \quad v_\theta^{(1)} = U \sin\theta.$$

Substituting the previous values of $\mathbf{n}$ and $\mathbf{s}$ into the Eq. (3.1) to (3.4), we have boundary conditions in a dimensionless form as

At $r = 1 + \alpha_m \vartheta_m(\zeta)$

$$v_r^{(1)} - v_r^{(2)} = \alpha_m \sqrt{1-\zeta^2} P_{m-1}(\zeta)(v_\theta^{(1)} - v_\theta^{(2)}), \tag{3.5}$$

$$t_{r\theta}^{(1)} + \alpha_m \sqrt{1-\zeta^2} P_{m-1}(\zeta)(t_{rr}^{(1)} - t_{\theta\theta}^{(1)}) = \frac{\xi_1}{\lambda}(v_\theta^{(1)} + v_r^{(1)} \alpha_m \sqrt{1-\zeta^2} P_{m-1}(\zeta)), \tag{3.6}$$

$$t_{rr}^{(1)} - 2\alpha_m \sqrt{1-\zeta^2} P_{m-1}(\zeta) t_{r\theta}^{(1)} = -p^{(2)}, \tag{3.7}$$

and $r = \eta[1 + \alpha_m \vartheta_m(\zeta)]$, where $\eta = b/a$,

$$v_r^{(2)} - \alpha_m \sqrt{1-\zeta^2} P_{m-1}(\zeta) v_\theta^{(2)} = 0. \tag{3.8}$$

In relation with stream functions $\psi^{(i)}$, $i = 1, 2$, the expressions is found as

$$\left(\frac{\partial\psi^{(1)}}{\partial\zeta} - \frac{\partial\psi^{(2)}}{\partial\zeta}\right) = r\alpha_m P_{m-1}(\zeta)\left(\frac{\partial\psi^{(1)}}{\partial r} - \frac{\partial\psi^{(2)}}{\partial r}\right), \tag{3.9}$$

$$\begin{aligned} 2r\frac{\partial}{\partial r}\left(\frac{1}{r}\frac{\partial\psi^{(1)}}{\partial r}\right) - E^2\psi^{(1)} \\ + 2\alpha_m\vartheta_2(\zeta)P_{m-1}(\zeta)\left(\frac{4}{r}\frac{\partial^2\psi^{(1)}}{\partial r\partial\zeta} - \frac{6}{r^2}\frac{\partial\psi^{(1)}}{\partial\zeta} + \frac{P_1(\zeta)}{r\vartheta_2(\zeta)}\frac{\partial\psi^{(1)}}{\partial r}\right) \\ = \frac{\xi_1}{\lambda}\left(\frac{\partial\psi^{(1)}}{\partial r} + \frac{1}{r}(1-\zeta^2)\alpha_m P_{m-1}(\zeta)\frac{\partial\psi^{(1)}}{\partial\zeta}\right), \end{aligned} \tag{3.10}$$

$$\begin{aligned} -p^{(1)} - \frac{2}{r^2}\left[\frac{2}{r}\frac{\partial\psi^{(1)}}{\partial\zeta} - \frac{\partial^2\psi^{(1)}}{\partial r\partial\zeta}\right] \\ - \frac{2\alpha_m P_{m-1}(\zeta)}{r}\left[2r\frac{\partial}{\partial r}\left(\frac{1}{r}\frac{\partial\psi^{(1)}}{\partial r}\right) - E^2\psi^{(1)}\right] = -p^{(2)}, \end{aligned} \tag{3.11}$$

$$\frac{\partial\psi^{(2)}}{\partial\zeta} = \alpha_m r P_{m-1}(\zeta)\frac{\partial\psi^{(2)}}{\partial r}. \tag{3.12}$$

4. Mathematical solution

The solutions for the fluid movement in region I and the permeable area (region II) after solving Eqs. (2.23) and (2.24) are

$$\begin{aligned} \psi^{(1)} = \left[r^2 + \frac{a_2}{r} + b_2\sqrt{r}K_{3/2}(\alpha r)\right]\vartheta_2(\zeta) \\ + \sum_{n=3}^{\infty}\left[A_n r^{-n+1} + B_n\sqrt{r}K_{n-1/2}(\alpha r)\right]\vartheta_n(\zeta), \end{aligned} \tag{4.1}$$

$$\psi^{(2)} = \left[c_2 r^2 + \frac{d_2}{r}\right]\vartheta_2(\zeta) + \sum_{n=3}^{\infty}[C_n r^n + D_n r^{-n+1}]\vartheta_n(\zeta). \tag{4.2}$$

The pressure for each of the flows are

$$p^{(1)} = \alpha^2\left[\left(r - \frac{a_2}{2r^2}\right)P_1(\zeta) - \sum_{n=3}^{\infty}\frac{A_n r^{-n}}{n}P_{n-1}(\zeta)\right], \tag{4.3}$$

$$p^{(2)} = \beta^2\left[\left(c_2 r - \frac{d_2}{2r^2}\right)P_1(\zeta) + \sum_{n=3}^{\infty}\left[C_n\frac{r^{n-1}}{n-1} - \frac{D_n r^{-n}}{n}\right]P_{n-1}(\zeta)\right]. \tag{4.4}$$

Inserting expressions (4.1) to (4.4) into the approximate boundary conditions (3.9) to (3.12), we acquire four equations in four unknown constants that are

presented in Appendix A. They are enough to decide the unknown constants of the favoured order for approximation, $O(\alpha_m)$. Thus, the stream functions for the flow field can be found up to $O(\alpha_m)$ [25].

Also, it is noteworthy that considering the case of flow past a permeable sphere with a solid core the coefficients which make a contribution to this flow case are a_2, b_2, c_2, d_2, and the rest of the coefficients must be zero which shows that the rest of the coefficients in Eqs. (4.1) and (4.2) are of the order $O(\alpha_m)$. Now, by evaluating the leading terms of systems of Eqs. (A.1) to (A.4) given in Appendix A, we obtain the arbitrary constants a_2 to d_2. Further, to find these arbitrary constants, we used the perturbation process to find the rest of the non-vanishing coefficients A_n, B_n, C_n, and D_n appearing in Eqs. (A.9) to (A.12) which corresponds to $n = m - 2$, m, $m + 2$.

At first, the results that deal with the boundaries $r = 1 + \alpha_m \vartheta_m(\zeta)$ and $r = \eta[1 + \alpha_m \vartheta_m(\zeta)]$ are obtained. Comparing Eqs. (4.1) and (4.2) with the expressions that arise in analysing the flow of viscous fluid past a permeable spherical particle with a core, suggests that the terms consisting of A_n, B_n, C_n and D_n for the case $n > 2$ are extra and does not exist in the flow past a permeable sphere with a core. Thus, all these coefficients must be of $O(\alpha_m)$. Presently, the movement of fluid past a particle with spheroidal geometry that slightly deviates from the spherical shape is considered. Thus, the motion of fluid past a spheroidal particle is anticipated to be moderately varying from the flow past a sphere. Therefore, when executing the boundary conditions, the deviations from the spherical form is neglected and put $r = 1$ in (3.9) to (3.11) for the terms involving A_n, B_n, C_n, D_n, and for $r = \eta$ in Eq. (3.12) for the terms C_n, D_n for $n > 2$.

The case in which the spheroid is represented by the boundaries

$$r = 1 + \sum_{m=2}^{\infty} \alpha_m \vartheta_m(\zeta), \tag{4.5}$$

and

$$r = \eta[1 + \sum_{m=2}^{\infty} \alpha_m \vartheta_m(\zeta)]. \tag{4.6}$$

We implement the similar process for all m's and the stream functions of the problem is obtained.

5. Spheroidal case

A specific case of the mentioned flow is the study of the movement through a permeable prolate and an oblate spheroid with a rigid core in the influence of a magnetic field.

In the Cartesian coordinate system, the spheroidal surface is

$$\frac{x^2+y^2}{c^2}+\frac{z^2}{c^2(1-\epsilon)^2}=1, \tag{5.1}$$

where c and ϵ are equatorial radius and non-sphericity parameter, respectively. The value of ϵ is considerably small that the squares and higher powers of it can be overlooked. After neglecting the quantities of $O(\epsilon^2)$ [74], in a polar coordinate system, Eq. (5.1) can be expressed as

$$r=a[1+2\epsilon\vartheta_2(\zeta)], \tag{5.2}$$

where $a=c(1-\epsilon)$ and $\vartheta_2(\zeta)=(\sin^2\theta)/2$.

For $0<\epsilon\leq 1$, the surface Eq. (5.2) represents an oblate spheroid and is a prolate spheroid for $\epsilon<0$. Further, $\epsilon=0$, resembles the equation of the sphere bearing radius c. This specific condition makes our problem quite easy to find the solution. To apply the above results, we choose $m=2$; $\alpha_m=2\epsilon$. For $m=2$, the constants A_0, B_0, C_0, D_0, will vanish.

The expression for the stream functions using Appendix C are now given as

$$\begin{aligned}\psi^{(1)}&=[r^2+(a_2+A_2)r^{-1}+(b_2+B_2)\sqrt{r}K_{3/2}(\alpha r)]\vartheta_2(\zeta)\\&\quad+[A_4r^{-3}+B_4\sqrt{r}K_{7/2}(\alpha r)]\vartheta_4(\zeta),\end{aligned} \tag{5.3}$$

$$\psi^{(2)}=[(c_2+C_2)r^2+(d_2+D_2)r^{-1}]\vartheta_2(\zeta)+[C_4r^4+D_4r^{-3}]\vartheta_4(\zeta), \tag{5.4}$$

and the pressure terms are

$$p^{(1)}=\alpha^2\left[\left(r-\left(\frac{a_2+A_2}{2r^2}\right)\right)P_1(\zeta)-\frac{A_4}{4r^4}P_3(\zeta)\right], \tag{5.5}$$

$$p^{(2)}=\beta^2\left[\left((c_2+C_2)r-\left(\frac{d_2+D_2}{2r^2}\right)\right)P_1(\zeta)+\left(C_4\frac{r^3}{3}-\frac{D_4}{4r^4}\right)P_3(\zeta)\right]. \tag{5.6}$$

6. Hydrodynamic drag

The flow of magneto-viscous fluid produces a resisting force on the spheroidal particle and this force (drag force) can be evaluated as [29, 33, 59, 72]

$$F_D=\int\limits_S(\mathbf{n}\cdot t^{(1)})\cdot\mathbf{k}\,dS, \tag{6.1}$$

where $\mathbf{n}=\mathbf{e}_r-\epsilon\sin 2\theta\mathbf{e}_\theta$; $dS=2\pi a^2(1+2\epsilon\sin^2\theta)\sin\theta d\theta$; $\mathbf{k}$ is the unit vector working in the z direction. Integrating over the surface of the body

$$r=1+2\epsilon\vartheta_2(\zeta)=1+\epsilon\sin^2\theta$$

(in non-dimensional form), we have

$$F_D = 2\pi a^2 \times \int_0^{\pi} r^2[(t_{rr} - \epsilon t_{\theta r}\sin 2\theta)\cos\theta - (t_{r\theta} - \epsilon t_{\theta\theta}\sin 2\theta)\sin\theta]|_{r=1+\epsilon\sin^2\theta}\sin\theta d\theta. \tag{6.2}$$

Simplification, using the stress components and stream function presented in Eq. (5.3), we derived the following [66, 68]

$$F_D = \frac{2}{3}\pi\mu U a\alpha^2\Bigg[a_2 + A_2 - 2 - 2(b_2 + B_2)K_{3/2}(\alpha) + \frac{4\epsilon}{5}\left(-5 + a_2 + \frac{b_2}{\alpha+1}(2\alpha^2 + \alpha + 1)K_{3/2}(\alpha)\right)\Bigg]. \tag{6.3}$$

The values of a_2, b_2, A_2, and B_2 are obtained by using the steps mentioned in Appendix A.

Utilising the above values and considering $a = c(1-\epsilon)$ and thereafter $\eta = \eta_1(1+\epsilon)$, $\alpha = \alpha_1(1-\epsilon)$, $\xi = \xi_1(1-\epsilon)$, $\chi = \chi_1(1-\epsilon)$, tending to $\beta = \beta_1(1-\epsilon)$, the ultimate equation is obtained. Also, $\eta_1 = b/c$ is the separation parameter (the measure of closeness between the porous spheroidal particle and the core),

$$\alpha_1 = \sqrt{\frac{\mu_h^2 H_o^2 \sigma c^2}{\mu}}, \quad \beta_1^2 = \xi_1^2 + \chi_1^2, \quad \chi_1 = \sqrt{\frac{\mu_h^2 H_o^2 \sigma c^2}{\varepsilon\mu}}, \quad \xi_1^2 = \frac{c^2}{k}, \quad k_1 = \xi_1^{-2}.$$

Therefore, the required drag is given below

$$F_D = \pi\mu U c\left[\frac{-(\delta_1\chi_1 + \delta_2\lambda)}{\nu_5\chi_1 + \lambda(\nu_7 + \eta_1{}^3\nu_6)} + \frac{\epsilon(\delta_3{\chi_1}^2 + \delta_4\lambda\chi_1 + \delta_5\lambda^2)}{\delta_6\lambda\chi_1 + \delta_7\lambda^2 + \delta_8}\right]. \tag{6.4}$$

The expressions for symbols ν_{i_1}, $i_1 = 1, \ldots, 29$, and δ_{j_1}, $j_1 = 1, \ldots, 8$ are mentioned in Appendix C.

Some special results

For validation of our result, a comparison of reduction cases with the previously published results is shown below:

Under magnetic effect

Case 1: In absence of impermeable core i.e., $\eta_1 = 0$, the MHD flow past a permeable spheroid is achieved and the drag expression is given as

$$F_D = -4\pi\mu U c\left[\frac{((\beta_1{}^2 + 4)\xi_1\omega_2 + \beta_1{}^2\lambda\Delta_3)}{\lambda\Delta_4 + \xi_1(\omega_1 + 2\beta_1{}^2)} - \frac{\epsilon\Delta_1}{4\Delta_2}\right]. \tag{6.5}$$

The introduced symbols ω_{i_2}, $i_2 = 1, \ldots, 17$, Δ_{j_2}, $j_2 = 1, \ldots, 13$, and Γ are mentioned in Appendix B.

Case 2: In absence of slip i.e., $\lambda = 0$ in Eq. (6.5), it acts as the MHD flow through a semipermeable spheroid and the drag expression leads to

$$F_D = -4\pi\mu U c\left[\frac{(\beta_1{}^2 + 4)\omega_2}{\omega_1 + 2\beta_1{}^2} - \frac{\epsilon\Gamma}{20\omega_4}\right]. \tag{6.6}$$

Case 3: Considering the case for non-sphericity parameter $\epsilon = 0$ in Eq. (6.5), it acts as MHD flow past a permeable sphere and the drag is

$$F_D = -4\pi\mu U c\left[\frac{((\beta_1{}^2 + 4)\xi_1\omega_2 + \beta_1{}^2\lambda\Delta_3)}{\lambda\Delta_4 + \xi_1(\omega_1 + 2\beta_1{}^2)}\right]. \tag{6.7}$$

Case 4: Further, supposing $\epsilon = 0$ in Eq. (6.6), it reduces to MHD flow past a semipermeable sphere and the obtained drag is

$$F_D = -4\pi\mu U c\left[\frac{(\beta_1{}^2 + 4)\omega_2}{\omega_1 + 2\beta_1{}^2}\right]. \tag{6.8}$$

Case 5: If $\xi_1 \to \infty$ and $\beta_1 \to \infty$ in Eq. (6.5), it behaves as a MHD flow past a solid spheroid and the drag is

$$F_D = -2\pi\mu U c\left[\omega_2 - \frac{3\omega_3\epsilon}{5}\right]. \tag{6.9}$$

It is in accordance with the work of Prasad and Bucha [66].

Case 6: For a non-sphericity parameter $\epsilon = 0$ in Eq. (6.9), it behaves as MHD flow past a rigid sphere. The drag so obtained is

$$F_D = -2\pi\mu U c\omega_2, \tag{6.10}$$

which acknowledge the works of Prasad and Bucha [60, 64].

Without magnetic effect

Case 1: If $\alpha_1 = 0$ and $\chi_1 = 0$ (i.e., $\beta_1 \to \xi_1$) in the expression of drag on MHD flow past a permeable spheroid with an impermeable core, we obtain the flow in absence of MHD effect and the drag reduces to

$$F_D = -6\pi\mu U c\left[\frac{2(\eta_1{}^3 + 2)\lambda\xi_1{}^2 + \Delta_{12}\xi_1}{3\lambda(2(\xi_1{}^2 + 3) + \eta_1{}^3(\xi_1{}^2 - 6)) + \Delta_{13}\xi_1} - \frac{\epsilon(\Delta_{11}\xi_1{}^2 + 6\Delta_9\lambda\xi_1 - 6\Delta_{10}\lambda^2)}{5(\Delta_7{}^2\xi_1{}^2 + 6\Delta_7\Delta_8\lambda\xi_1 + 9\Delta_8{}^2\lambda^2)}\right]. \tag{6.11}$$

For $\epsilon = 0$, the flow past a permeable sphere with a core is obtained.

Case 2: If $\lambda = 0$ in Eq. (6.11), we obtain the flow past a semipermeable spheroid with an impermeable core and the drag is

$$F_D = -6\pi\mu U c\left[\frac{\Delta_{12}}{\Delta_{13}} - \frac{\epsilon}{5}\frac{\Delta_{11}}{{\Delta_7}^2}\right]. \tag{6.12}$$

For $\epsilon = 0$, the flow past a semipermeable sphere with a core is obtained.

Case 3: If $\alpha_1 = 0$ and $\chi_1 = 0$ (i.e., $\beta_1 \to \xi_1$) in Eq. (6.5), it acts as the flow past a permeable spheroid and the drag expression reduces to

$$F_D = -4\pi\mu U c\left[\frac{3\xi_1(2\xi_1\lambda + \xi_1^2 + 4)}{(6{\xi_1}^2 + 18)\lambda + 2{\xi_1}^3 + 9\xi_1} + \frac{\epsilon\Delta_5}{\Delta_6}\right]. \tag{6.13}$$

Case 4: Considering no slip i.e., $\lambda = 0$ in Eq. (6.13), it leads to the flow past a semipermeable spheroid. Now the drag is expressed as

$$F_D = 6\pi\mu U c\left[\frac{2(({\xi_1}^2 + 12)(2{\xi_1}^2 + 5)\epsilon - 5({\xi_1}^2 + 4)(2{\xi_1}^2 + 9))}{5(2{\xi_1}^2 + 9)^2}\right]. \tag{6.14}$$

Case 5: If the non-sphericity parameter reduces to $\epsilon = 0$ in Eq. (6.13), the flow past a permeable sphere is achieved and the drag is

$$F_D = -6\pi\mu U c\left[\frac{4\xi_1^2\lambda + \xi_1(2{\xi_1}^2 + 8)}{(6{\xi_1}^2 + 18)\lambda + \xi_1(2{\xi_1}^2 + 9)}\right]. \tag{6.15}$$

Case 6: Eq. (6.15) along with $\lambda = 0$ reduces to the flow past a semipermeable sphere. The drag is expressed as

$$F_D = -6\pi\mu U c\left[\frac{2{\xi_1}^2 + 8}{2{\xi_1}^2 + 9}\right]. \tag{6.16}$$

Case 3 to 6 are in acknowledgement to the result of PRASAD and BUCHA [43].

Case 7: If $\xi_1 \to \infty$ (permeability $k = 0$) in Eq. (6.14), it acts as a flow past a solid spheroid. The obtained drag is

$$F_D = -6\pi\mu U c\left[1 - \frac{\epsilon}{5}\right], \tag{6.17}$$

which is in support to the renowned Stokes for viscous flow past a solid spheroid [72].

Case 8: If $\xi_1 \to \infty$ (permeability $k = 0$) in Eq. (6.16), it behaves as flow past a solid sphere and the drag is

$$F_D = -6\pi\mu U c, \tag{6.18}$$

which is the famous Stokes drag expression for viscous flow through a rigid sphere [72].

7. Numerical representation and discussion

The profiles of the drag coefficient are presented in Figs. 2–13. The drag coefficient D_N is mathematically denoted as

$$D_N = \frac{F_D}{-6\pi\mu Uc}.$$

As the work under consideration involves several non-dimensional parameters which are importantly used for the numerical calculation, therefore we mention them specifically as:

1. Hartmann number for fluid region (α_1).
2. Hartmann number for permeable region (χ_1).
3. Slip parameter (λ).
4. Non-sphericity parameter (ϵ).
5. Non-dimensional permeability parameter (k_1).
6. Separation parameter (η_1).

In all the computation the Hartmann number for a fluid region is chosen to be $\alpha_1 \geq 0$ [59], the Hartmann number for permeable region $\chi_1 \geq 0$ [59], slip parameter $0.25 \leq \lambda \leq 10$ [6, 38, 43, 73], non-sphericity parameter $0 < \epsilon \leq 1$ for an oblate spheroid and $\epsilon < 0$ for a prolate spheroid [25, 29, 43], non-dimensional permeability parameter $k_1 \geq 0$, separation parameter $0 < \eta_1 < 1$ as $\eta_1 = b/c$ which is the ratio of the radius of an inner core to the radius of outer spheroid which cannot exceed one.

The variation of D_N against the permeability parameter addressing the impact of numerous important parameters is mentioned in Figs. 2 to 6. The plots corresponding to the variation of the coefficient of drag with the different Hartmann number α_1 of the fluid region are figured out in Fig. 2, for both the case of a prolate ($\epsilon = -0.3$) as well as an oblate ($\epsilon = 0.3$) permeable spheroid with an impermeable core, by fixing slip value as $\lambda = 3$ and the Hartmann number ($\chi_1 = 5$) and $\eta_1 = 0.6$. Besides, Fig. 3 demonstrates the alteration of the coefficient of drag for advancing the Hartmann number α_1 for both prolate and oblate semipermeable spheroid with an impermeable core. It follows that for enhancing value of the Hartmann number α_1, the coefficient of drag also advances. The reason behind the same is the applied magnetic field that generates a retarding force, i.e., the Lorentz force, and as this force increases, it suppresses the rate of flow which decreases the velocity, and thus an increase in the drag is observed. Additionally, it is worth noticing that D_N for the flow past permeable spheroidal particle with the core is lower as compared to the semipermeable spheroid with a core, which indicates the comparative ease of flow in the permeable spheroidal case.

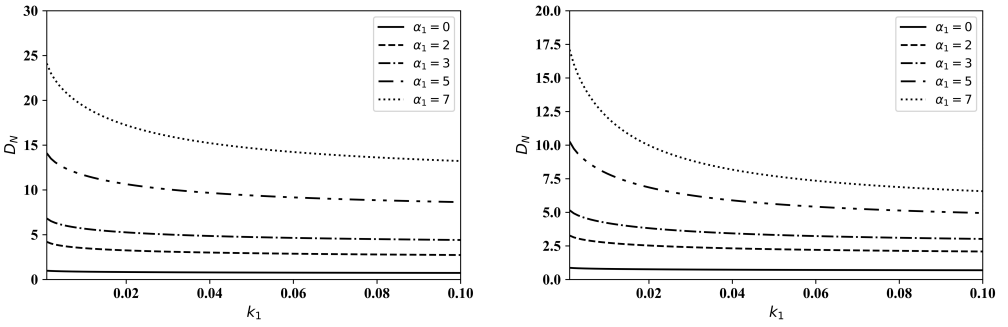

a) $\epsilon = -0.3$ b) $\epsilon = 0.3$

FIG. 2. Coefficient of drag plotted against permeability parameter k_1 for increasing Hartmann number α_1 with fixed parameters $\chi_1 = 5$, $\lambda = 3$, $\eta_1 = 0.6$.

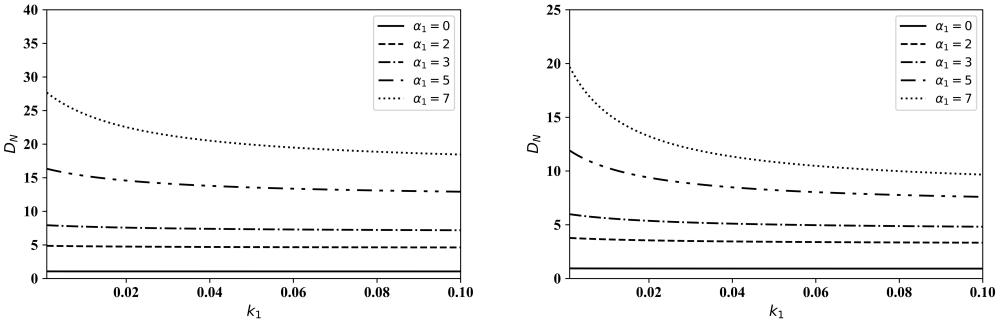

a) $\epsilon = -0.3$ b) $\epsilon = 0.3$

FIG. 3. Coefficient of drag plotted against permeability parameter k_1 for increasing Hartmann number α_1 with fixed parameters $\chi_1 = 5$, $\lambda = 0$, $\eta_1 = 0.6$.

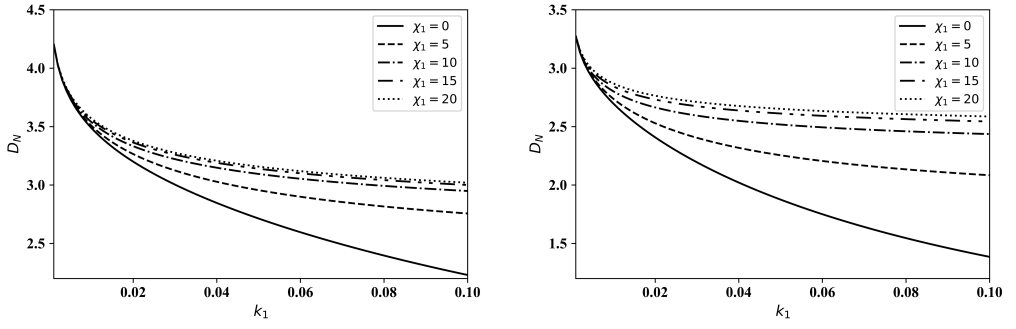

a) $\epsilon = -0.3$ b) $\epsilon = 0.3$

FIG. 4. Coefficient of drag plotted against permeability parameter k_1 for increasing Hartmann number χ_1 with fixed parameters $\alpha = 2$, $\lambda = 3$, $\eta_1 = 0.6$.

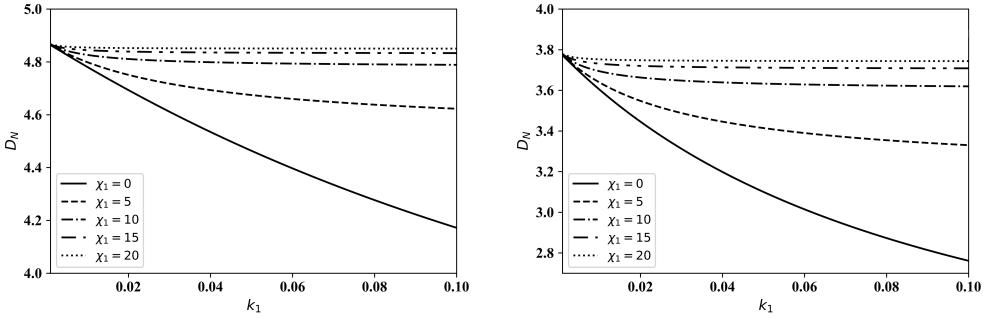

a) $\epsilon = -0.3$ b) $\epsilon = 0.3$

Fig. 5. Coefficient of drag plotted against permeability parameter k_1 for increasing Hartmann number χ_1 with fixed parameters $\alpha_1 = 2$, $\lambda = 0$, $\eta_1 = 0.6$.

All the curves in Figs. 4 and 5 portray the nature of the drag coefficient for the varying Hartmann number χ_1 of the permeable region corresponding to the permeable and semipermeable spheroid with a solid core, respectively. The increase of the Hartmann number χ_1 implies the intensification of the magnetic effect in the porous region which leads to higher values of the drag force. Furthermore, the curves for both oblate and prolate spheroids point out the greater resistance on a prolate spheroid as compared to an oblate spheroid. Again, as expected, the figures discussed show a decrease in resistance as the permeability increases.

The drag coefficient for the variation in the value of the non-sphericity parameter is shown in Fig. 6 which illustrates that the drag decreases monotonically with enhancing a non-sphericity parameter. The graph for $\epsilon = 0$ indicates the case for the flow past a spherical particle with a core and it is observed that the resistance on the spherical particles is greater than that of the oblate spheroid but less than the resistance exerted by the prolate spheroid.

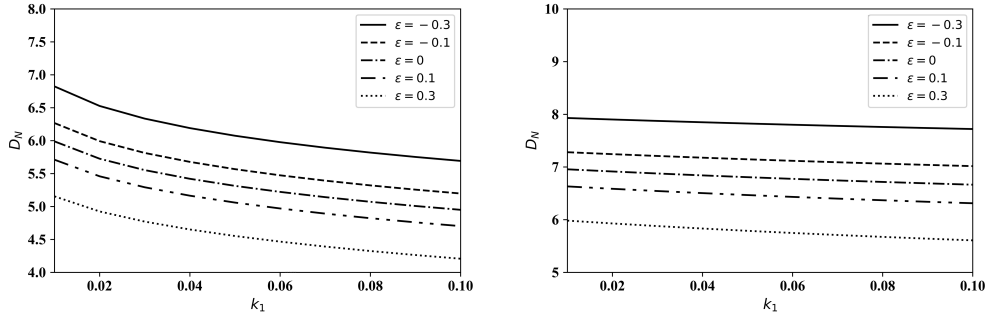

a) $\lambda = 3$ b) $\lambda = 0$

Fig. 6. Coefficient of drag plotted against permeability parameter k_1 for increasing non-sphericity parameter ϵ with fixed parameters $\alpha_1 = 3$, $\chi_1 = 5$, $\eta_1 = 0.6$.

Figure 7 depicts the variation of drag with the varying separation parameter η_1 for the case of prolate spheroid ($\epsilon = -0.3$) with $\lambda = 1$ and $\lambda = 0$, respectively and η_1 represents the measure of closeness between the porous particle and the core, and it varies from 0 to 1. As η_1 approaches 1, i.e., the distance between the core and the porous region's boundary decreases and the porous particle with a core behaves as a solid particle. For η_1 tending to 0, the porous particle with a rigid core behaves as a porous particle without the core. The drag for the prolate spheroid is observed to be decreasing with increasing η_1 (i.e., reducing the porous region's thickness).

Figure 8 portrays the variation of drag against the varying separation parameter η_1 for $\epsilon = 0.3$ oblate spheroid with $\lambda = 1$ and $\lambda = 0$, respectively. It has been noticed that when the value of η_1 rises, so does the drag on the oblate spheroid with an impermeable core.

Observation of the drag coefficient for enhancing α_1 is pictured in Fig. 9 for altering values of slip. For the entire range of slip, the drag is noted to be an increasing function of the magnetic parameter α_1. In a similar way, Fig. 10 analyzes the plots of D_N for different values of χ_1. The result shows the increase in the resisting force acting on both the prolate and oblate spheroid for a higher magnetic effect in the permeable region. For a particular value of χ_1, the drag is found to be decreasing with an increase in slip. It is important to note that all the curves representing the cases without magnetic effects are in support of the results obtained in [43].

Figure 11 shows the drag coefficient profile for various values of ϵ with varying slip (λ) for (a) the presence of magnetic forces ($\alpha_1 = 2$, $\chi_1 = 5$) and (b) without the magnetic forces ($\alpha_1 = 0$,$\chi_1 = 0$). Both the graphs clearly show that the occurrence of the transverse magnetic field opposes the transport process which in turn produces more resistance to flow than the flow without the MHD effect, and therefore enhances the drag acting to a higher extent. Also, from the discussed figures one can observe that the rate of flow is increased for increasing non-sphericity parameters.

Figures 12 and 13 show the effect of η_1, λ, ϵ on the drag coefficient both in presence and absence of magnetic influence. It is clear from the figure that for $\epsilon = 0.3$, the drag increases as η_1 increases but for $\epsilon = -0.3$, the drag reduces as η_1 increases. From both the figures it is clear that the parameters η_1, λ, ϵ show similar change in behavior but applying magnetic forces, the effect of all the parameters are enhanced. Therefore, resistance to the flow past a permeable spheroid with the MHD effect is larger than the flow without magnetic effect, and similar results are found for the case of the semipermeable spheroid. Moreover, all the obtained results emphasize the importance of introducing magnetic forces during the study of mentioned flows.

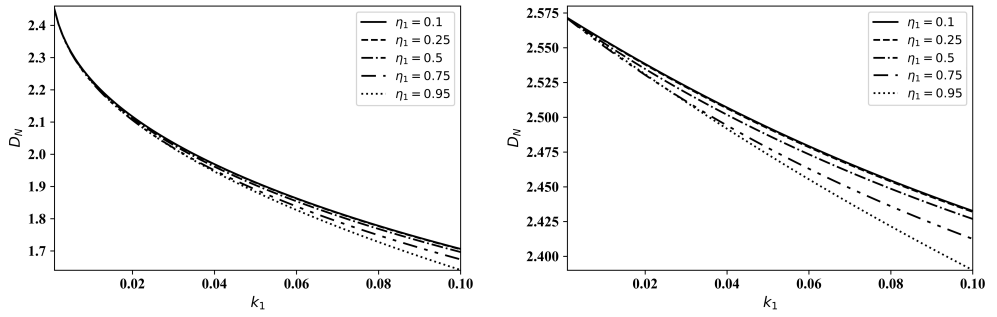

a) $\lambda = 1$ b) $\lambda = 0$

Fig. 7. Coefficient of drag plotted against permeability parameter k_1 for increasing separation parameter η_1 with fixed parameters $\alpha_1 = 1$, $\chi_1 = 1$, $\epsilon = -0.3$.

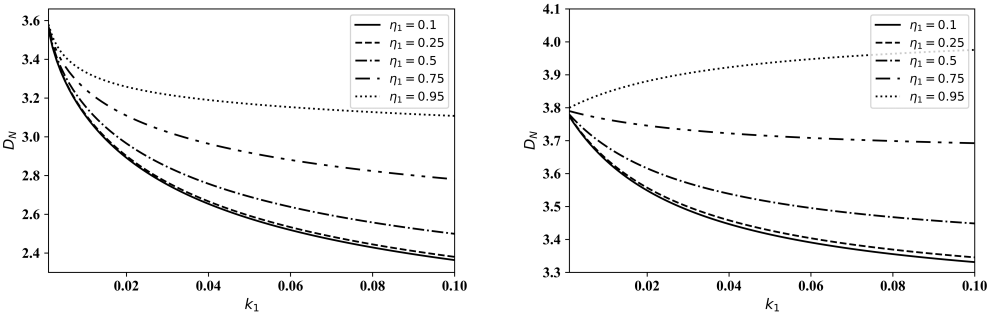

a) $\lambda = 1$ b) $\lambda = 0$

Fig. 8. Coefficient of drag plotted against permeability parameter k_1 for increasing separation parameter η_1 with fixed parameters $\alpha_1 = 2$, $\chi_1 = 5$, $\epsilon = 0.3$.

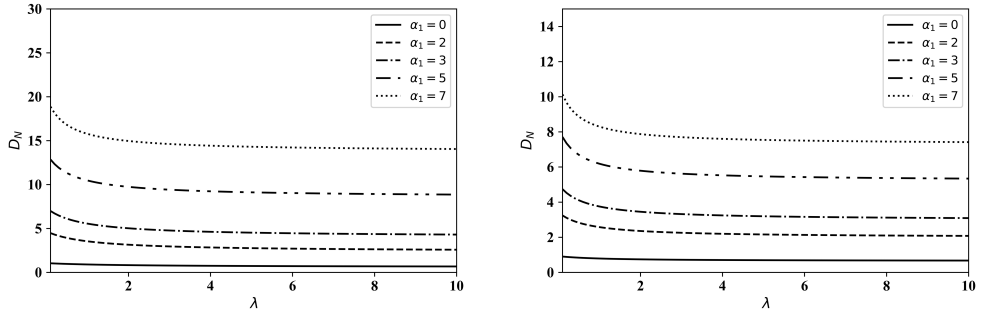

a) $\epsilon = -0.3$ b) $\epsilon = 0.3$

Fig. 9. Coefficient of drag plotted against slip parameter λ for increasing Hartmann number α_1 with fixed parameters $\chi_1 = 5$, $k_1 = 0.05$, $\eta_1 = 0.6$.

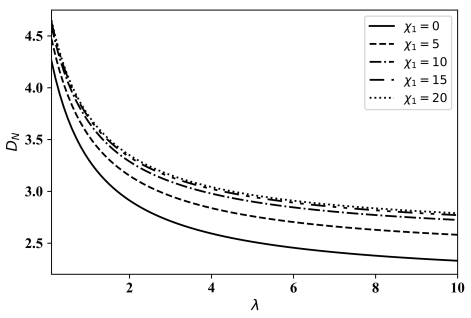

a) $\epsilon = -0.3$

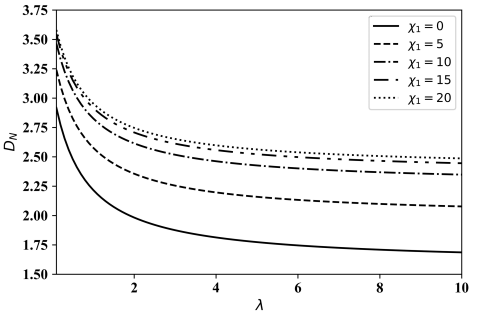

b) $\epsilon = 0.3$

FIG. 10. Coefficient of drag plotted against slip parameter λ for increasing Hartmann number χ_1 with fixed parameters $\alpha_1 = 2$, $k_1 = 0.05$, $\eta_1 = 0.6$.

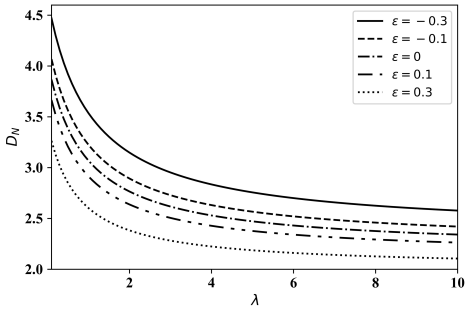

a) $\alpha_1 = 2$, $\chi_1 = 5$

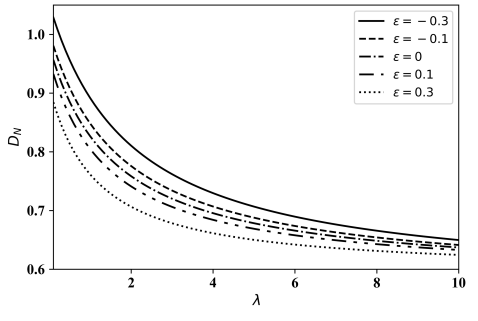

b) $\alpha_1 = 0$, $\chi_1 = 0$

FIG. 11. Coefficient of drag plotted against slip parameter λ for increasing non-sphericity parameter ϵ with fixed parameters $k_1 = 0.05$, $\eta_1 = 0.3$.

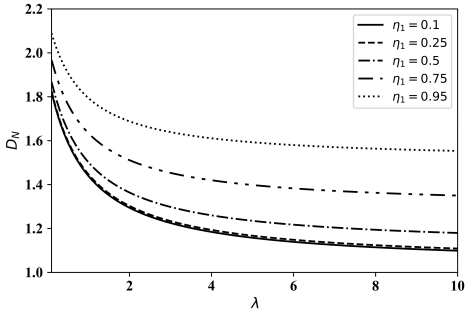

a) $\epsilon = -0.3$

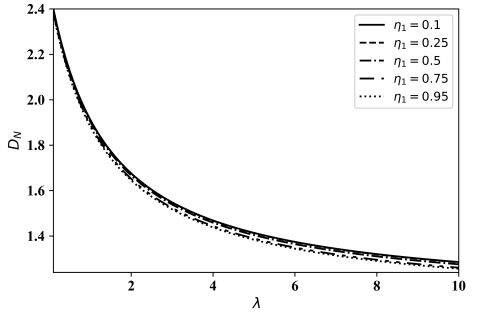

b) $\epsilon = 0.3$

FIG. 12. Coefficient of drag plotted against slip parameter λ for increasing separation parameter η_1 with fixed parameters $\alpha_1 = 1$, $\chi_1 = 1$, $k_1 = 0.05$.

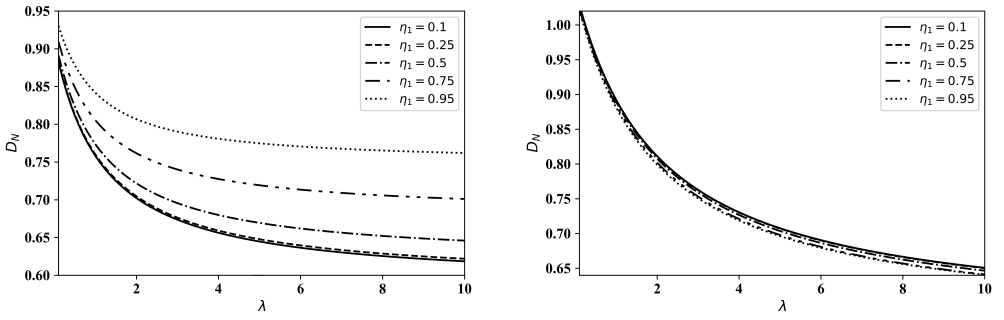

a) $\epsilon = -0.3$ b) $\epsilon = 0.3$

Fig. 13. Coefficient of drag plotted against slip parameter λ for increasing separation parameter η_1 with fixed parameters $\alpha_1 = 0$, $\chi_1 = 0$, $k_1 = 0.05$.

8. Conclusions

The current study shows light on the viscous incompressible fluid's motion, passing through a spheroidal particle of a permeable structure with an impermeable core when magnetic forces are present. An analytical solution to the problem, governed by Stokes and Darcy's law, has been examined. Beavers–Joseph–Saffman–Jones boundary condition accompanying the continuity of normal velocities and the balance of the pressure and normal stresses is supposed to be applicable at the fluid porous interface along with vanishing of the normal component of velocity at the surface of the impermeable core. The study also surveys the influence of relevant parameters on the flow dynamics, using a numerical approach.

The conclusions drawn from the present analysis are as follow:

- An expression for drag that a permeable spheroid with the solid core experiences is computed by adopting the analytical technique and important results are deduced, which are consistent with the earlier observations available in the literature.
- It is worth noticing the drag coefficient to be a rising function of the Hartmann numbers (α_1, χ_1) and a reducing function of permeability k_1, the non-sphericity parameter ϵ, slip parameter λ.
- The drag is discovered to be an increasing and a decreasing function of a separation parameter for the oblate and prolate spheroid with a core, respectively.
- Interestingly, the transverse magnetic field has an effect to retard the flow velocity, which leads to the increment of the drag forces.

- Based on the above analysis, it is effectively concluded that drag acting on permeable and semipermeable spheroids with an impermeable core under the MHD effect is higher as compared to the case without magnetic forces.
- As a result, supplying a magnetic field to the flow past permeable spheroid with the deformed core is found to have a considerable impact on the characteristic of fluid flow, and thus the proposed scheme is of much importance while dealing with MHD flow past deformed spherical particles.

Appendix A

In this appendix one can find the algebraic equations required for determining the coefficients given in Eqs. (4.1) and (4.2) and their solutions as well.

We get the following equations by applying the Eqs. (3.9) to (3.12) up to first order of α_m

$$
\begin{aligned}
(A.1)\quad & [1+a_2+b_2K_{3/2}(\alpha)-c_2-d_2]P_1(\zeta)\\
&\quad +\alpha_m[2-a_2-(K_{3/2}(\alpha)+\alpha K_{1/2}(\alpha))b_2-2c_2+d_2]Q(\zeta)\\
&+\sum_{n=3}^{\infty}[A_n+K_{n-1/2}(\alpha)B_n-C_n-D_n]P_{n-1}(\zeta)=0,\\
(A.2)\quad & \big[(6\lambda+\xi_1)a_2+(\lambda((\alpha^2+6)K_{3/2}(\alpha)+2\alpha K_{1/2}(\alpha))\\
&\quad +\xi_1(K_{3/2}(\alpha)+\alpha K_{1/2}(\alpha)))b_2-2\xi_1\big]\vartheta_2(\zeta)\\
&\quad +\alpha_m\vartheta_2(\zeta)[-((18\lambda+2\xi_1)a_2+(\lambda(\alpha^2+6)(3K_{3/2}(\alpha)+\alpha K_{1/2}(\alpha))\\
&\quad +\xi_1((\alpha^2+2)K_{3/2}(\alpha)))b_2+2\xi_1)\vartheta_m(\zeta)+((18\lambda+2\xi_1)a_2\\
&\quad +2(3\lambda(3K_{3/2}(\alpha)+\alpha K_{1/2}(\alpha))+\xi_1K_{3/2}(\alpha))b_2\\
&\quad +2\xi_1)P_1(\zeta)P_{m-1}(\zeta)]-\sum_{n=3}^{\infty}[(2(1-n^2)\lambda+\xi_1(1-n))A_n\\
&\quad +(\lambda((2(n^2-1)+\alpha^2)K_{n-1/2}(\alpha)+2\alpha K_{n-3/2})\\
&\quad +\xi_1((n-1)K_{n-1/2}(\alpha)+\alpha K_{n-3/2}(\alpha)))B_n]\vartheta_n(\zeta)=0,\\
(A.3)\quad & [(6+\alpha^2/2)a_2+2(3K_{3/2}(\alpha)+\alpha K_{1/2}(\alpha))b_2+\beta^2c_2\\
&-(\beta^2/2)d_2-\alpha^2]P_1(\zeta)-\alpha_m[(12+\alpha^2)a_2+2(6K_{3/2}(\alpha)+2\alpha K_{1/2}(\alpha))b_2\\
&-\beta^2c_2-\beta^2d_2+\alpha^2]\vartheta_m(\zeta)P_1(\zeta)-\alpha_m[12a_2+2((\alpha^2+6)K_{3/2}+2\alpha K_{1/2})b_2]Q(\zeta)\\
&+\sum_{n=3}^{\infty}[(2(n+1)+\alpha^2/n)A_n+(2((1+n)K_{n-1/2}+\alpha K_{n-3/2}))B_n\\
&+(\beta^2/(n-1))C_n-(\beta^2/n)D_n]P_{n-1}(\zeta)=0,
\end{aligned}
$$

$$(\eta^2 c_2+\eta^{-1}d_2)P_1(\zeta)+\alpha_m[2\eta^2 c_2-\eta^{-1}d_2]Q(\zeta) + \sum_{n=3}^{\infty}[C_n\eta^n+D_n\eta^{1-n}]P_{n-1}(\zeta) = 0, \tag{A.4}$$

where

$$Q(\zeta) = \vartheta_m(\zeta)P_1(\zeta) + \vartheta_2(\zeta)P_{m-1}(\zeta).$$

By equating the leading terms of Eqs. (A.1) to (A.4) to zero, we obtain

$$1 + a_2 + b_2K_{3/2}(\alpha) - c_2 - d_2 = 0, \tag{A.5}$$

$$(6\lambda + \xi_1)a_2 + (\lambda((\alpha^2 + 6)K_{3/2}(\alpha) + 2\alpha K_{1/2}(\alpha)) + \xi_1(K_{3/2}(\alpha) + \alpha K_{1/2}(\alpha)))b_2 - 2\xi_1 = 0, \tag{A.6}$$

$$(6 + \alpha^2/2)a_2 + 2(3K_{3/2}(\alpha) + \alpha K_{1/2}(\alpha))b_2 + \beta^2 c_2 - (\beta^2/2)d_2 - \alpha^2 = 0, \tag{A.7}$$

$$\eta^2 c_2 + \eta^{-1}d_2 = 0. \tag{A.8}$$

Solving these equations the values of a_2, b_2, c_2, and d_2 are obtained. Now, Eqs. (A.1) to (A.4) reduces to

$$\sum_{n=3}^{\infty}[A_n + K_{n-1/2}(\alpha)B_n - C_n - D_n]P_{n-1}(\zeta) + \alpha_m\Omega_1 Q(\zeta) = 0, \tag{A.9}$$

$$-\sum_{n=3}^{\infty}[(2(1-n^2)\lambda + \xi_1(1-n))A_n + (\lambda((2(n^2-1)+\alpha^2)K_{n-1/2}(\alpha) + 2\alpha K_{n-3/2}) + \xi_1((n-1)K_{n-1/2}(\alpha) + \alpha K_{n-3/2}(\alpha)))B_n]\vartheta_n(\zeta) + \alpha_m\vartheta_2(\zeta)[\Omega_2\vartheta_m(\zeta) + \Omega_3 P_1(\zeta)P_{m-1}(\zeta)] = 0, \tag{A.10}$$

$$\sum_{n=3}^{\infty}[(2(n+1)+\alpha^2/n)A_n + (2((1+n)K_{n-1/2} + \alpha K_{n-3/2}))B_n + \beta^2/(n-1)C_n - (\beta^2/n)D_n]P_{n-1}(\zeta) + \alpha_m\Omega_4\vartheta_m(\zeta)P_1(\zeta) - \alpha_m\Omega_5 Q(\zeta) = 0, \tag{A.11}$$

$$\sum_{n=3}^{\infty}[C_n\eta^n + D_n\eta^{1-n}]P_{n-1}(\zeta) + \alpha_m\Omega_6 Q(\zeta) = 0. \tag{A.12}$$

Again for finding the values A_n, B_n, C_n, and D_n, the identities (A.13)-(A.16) mentioned in Prasad and Bucha [66] are used in Eqs. (A.9) to (A.12), it is observed that the values of A_n, B_n, C_n, and D_n vanishes when $n \neq m-2, m, m+2$.

The expressions for $n = m-2, m, m+2$ are as follows

$$A_n + B_n K_{n-1/2} - C_n - D_n + \Omega_1 \overline{a}_n = 0, \tag{A.13}$$

$$\begin{aligned}(2(n^2-1)\lambda + \xi_1(n-1))A_n + (\lambda[(2(n^2-1)+\alpha^2)K_{n-1/2}(\alpha) \\ + 2\alpha K_{n-3/2}(\alpha)] + \xi_1[(n-1)K_{n-1/2}(\alpha) + \alpha K_{n-3/2}(\alpha)])B_n \\ + \Omega_2 \overline{a}_n + \Omega_3 \overline{b}_n = 0,\end{aligned} \tag{A.14}$$

$$\begin{aligned}(2(n+1)+\alpha^2/n)A_n + 2((1+n)K_{n-1/2}(\alpha) + \alpha K_{n-3/2}(\alpha))B_n \\ + (\beta^2/(n-1))C_n - (\beta^2/n)D_n + \Omega_4 \overline{c}_n - \Omega_5 \overline{a}_n = 0,\end{aligned} \tag{A.15}$$

$$\eta^n C_n + \eta^{1-n} D_n + \Omega_6 \overline{a}_n = 0, \tag{A.16}$$

where

$$\begin{aligned}\Omega_1 &= 2 - a_2 - (K_{3/2}(\alpha) + \alpha K_{1/2}(\alpha))b_2 - 2c_2 + d_2, \\ \Omega_2 &= -2(9\lambda + \xi_1)a_2 - [\lambda(\alpha^2+6)\{3K_{3/2}(\alpha) + \alpha K_{1/2}(\alpha)\} \\ &\quad + \xi_1(\alpha^2+2)K_{3/2}(\alpha)]b_2 - 2\xi_1, \\ \Omega_3 &= (18\lambda + 2\xi_1)a_2 + \{6\lambda(3K_{3/2}(\alpha) + \alpha K_{1/2}(\alpha)) + 2\xi_1 K_{3/2}(\alpha)\}b_2 + 2\xi_1, \\ \Omega_4 &= -(12+\alpha^2)a_2 - 4(3K_{3/2}(\alpha) + \alpha K_{1/2}(\alpha))b_2 + \beta^2 c_2 + \beta^2 d_2 - \alpha^2, \\ \Omega_5 &= 12a_2 + 2\{(6+\alpha^2)K_{3/2}(\alpha) + 2\alpha K_{1/2}(\alpha)\}b_2, \\ \Omega_6 &= 2\eta^2 c_2 - \eta^{-1} d_2,\end{aligned}$$

and

$$\begin{aligned}\overline{a}_n &= \frac{n(n-1)\alpha_n}{(2n+1)(2n-3)}, \\ \overline{b}_n &= \frac{n(n-1)\alpha_n}{2(2n+1)(2n-3)}, \\ \overline{c}_n &= \frac{\alpha_n}{(2n+1)(2n-3)}.\end{aligned} \tag{A.17}$$

Using all the above equations for simplifying (A.13) to (A.16), we obtain the individual expressions of A_n, B_n, C_n, and D_n for $n = m-2, m, m+2$.

Appendix B

The values of ω_{i_2}, $i_2 = 1, \ldots, 17$, Δ_{j_2}, $j_2 = 1, \ldots, 13$ and Γ are defined as:

$$\begin{aligned}\omega_1 &= \alpha_1^2 + \alpha_1 + 9, \\ \omega_2 &= \alpha_1^2 + 3\alpha_1 + 3, \\ \omega_3 &= \alpha_1^2 + 2\alpha_1 + 1,\end{aligned}$$

$$
\begin{aligned}
\omega_4 &= 4\beta_1^2(\omega_1+\beta_1^2)+\alpha_1(\alpha_1^3+2\alpha_1^2+19\alpha_1+18)+81,\\
\omega_5 &= 2\alpha_1^3+7\alpha_1^2+30\alpha_1+45,\\
\omega_6 &= \alpha_1^3+3\alpha_1^2+18\alpha_1+18,\\
\omega_7 &= \alpha_1^2+6\alpha_1+9,\\
\omega_8 &= \alpha_1(9\alpha_1^3+38\alpha_1^2+123\alpha_1+174)+87,\\
\omega_9 &= \alpha_1(3\alpha_1^3+14\alpha_1^2+57\alpha_1+90)+45,\\
\omega_{10} &= \alpha_1(9\alpha_1^4+46\alpha_1^3+234\alpha_1^2+561\alpha_1+684)+342,\\
\omega_{11} &= \alpha_1(\alpha_1^4+10\alpha_1^3+64\alpha_1^2+174\alpha_1+216)+108,\\
\omega_{12} &= (\alpha_1-1)\alpha_1(\alpha_1+6)-6,\\
\omega_{13} &= \alpha_1(3\alpha_1^5+18\alpha_1^4+107\alpha_1^3+264\alpha_1^2+372\alpha_1+360)+180,\\
\omega_{14} &= 10\omega_1\omega_6+20\beta_1^2\omega_5+40(\alpha_1+3)\beta_1^4,\\
\omega_{15} &= 5(4\beta_1^4\omega_7+\omega_6(\omega_6+4\alpha_1\beta_1^2+12\beta_1^2)),\\
\omega_{16} &= 8(6(\alpha_1+1)\beta_1^4\omega_2+6\omega_{11}+\beta_1^2\omega_{10}),\\
\omega_{17} &= 12\beta_1^2\omega_{13}+24(\alpha_1+1)\beta_1^4\omega_{12},\\
\Delta_1 &= \lambda^2\omega_{17}+\lambda\xi_1\omega_{16}+\Gamma{\xi_1}^2,\\
\Delta_2 &= 5\xi_1^2\omega_4+\lambda^2\omega_{15}+\lambda\xi_1\omega_{14},\\
\Delta_3 &= (\alpha_1^3+3\alpha_1^2+6\alpha_1+6),\\
\Delta_4 &= (\omega_6+(2\alpha_1+6)\beta_1^2),\\
\Delta_5 &= 3\xi_1(12\lambda(\xi_1^4-\lambda\xi_1^3+19\xi_1^2+15\lambda\xi_1+36)+\xi_1(\xi_1^2+12)(2\xi_1^2+5)),\\
\Delta_6 &= 5(2\xi_1^3+6\xi_1^2\lambda+9\xi_1+18\lambda)^2,\\
\Delta_7 &= \eta_1^3\xi_1^2+2\xi_1^2-9\eta_1^3+9,\\
\Delta_8 &= \eta_1^3\xi_1^2+2\xi_1^2-6\eta_1^3+6,\\
\Delta_9 &= 4(\xi_1^4+19\xi_1^2+36)+4\eta_1^3(\xi_1^4-35\xi_1^2-72)\\
&\quad +\eta_1^6(\xi_1^2-18)(\xi_1^2-8),\\
\Delta_{10} &= 4\eta_1^3\xi_1^2(\xi_1^2+84)+\eta_1^6\xi_1^2(\xi_1^2-6)+4\xi_1^2(\xi_1^2-15),\\
\Delta_{11} &= 4\eta_1^3(\xi_1^4-20\xi_1^2-60)+2(\xi_1^2+12)(2\xi_1^2+5)\\
&\quad +\eta_1^6(\xi_1^2-15)(\xi_1^2-8),\\
\Delta_{12} &= 2(\xi_1^2+4)+\eta_1^3(\xi_1^2-8),\\
\Delta_{13} &= 2\xi_1^2+\eta_1^3(\xi_1^2-9)+9,\\
\Gamma &= 4(4\omega_9+\beta_1^2(\omega_8+6\beta_1^2\omega_3)).
\end{aligned}
$$

Appendix C

The stream functions for both the flows in fluid region and within permeable spheroid are given by

$$\begin{aligned}(\text{C.1})\quad \psi^{(1)} &= \left[r^2+\frac{a_2}{r}+b_2\sqrt{r}K_{3/2}(\alpha r)\right]\vartheta_2(\zeta)\\ &\quad+[A_{m-2}r^{-m+3}+B_{m-2}\sqrt{r}K_{m-5/2}(\alpha r)]\vartheta_{m-2}(\zeta)\\ &\quad+[A_m r^{-m+1}+B_m\sqrt{r}K_{m-1/2}(\alpha r)]\vartheta_m(\zeta)\\ &\quad+[A_{m+2}r^{-m-1}+B_{m+2}\sqrt{r}K_{m+3/2}(\alpha r)]\vartheta_{m+2}(\zeta),\end{aligned}$$

$$\begin{aligned}(\text{C.2})\quad \psi^{(2)} &= \left[c_2r^2+\frac{d_2}{r}\right]\vartheta_2(\zeta)+\left[C_{m-2}r^{m-2}+D_{m-2}r^{-m+3}\right]\vartheta_{m-2}(\zeta)\\ &\quad+[C_m r^m+D_m r^{-m+1}]\vartheta_m(\zeta)+[C_{m+2}r^{m+2}+D_{m+2}r^{-m-1}]\vartheta_{m+2}(\zeta),\end{aligned}$$

and the pressure terms for the flows are given by

$$\begin{aligned}(\text{C.3})\quad p^{(1)} &= \alpha^2\left[\left(r-\frac{a_2}{2r^2}\right)P_1(\zeta)-\frac{A_{m-2}r^{-m+2}}{m-2}P_{m-3}(\zeta)-\frac{A_m r^{-m}}{m}P_{m-1}(\zeta)\right.\\ &\quad\left.-\frac{A_{m+2}r^{-m-2}}{m+2}P_{m+1}(\zeta)\right],\end{aligned}$$

$$\begin{aligned}(\text{C.4})\quad p^{(2)} &= \beta^2\left[\left(c_2r-\frac{d_2}{2r^2}\right)P_1(\zeta)+\left(C_{m-2}\frac{r^{m-3}}{m-3}-\frac{A_{m-2}r^{-m+2}}{m-2}\right)P_{m-3}(\zeta)\right.\\ &\quad+\left(C_m\frac{r^{m-1}}{m-1}-\frac{A_m r^{-m}}{m}\right)P_{m-1}(\zeta)+\left(C_{m+2}\frac{r^{m+1}}{m+1}-\frac{A_{m+2}r^{-m-2}}{m+2}\right)P_{m+1}(\zeta)\left.\right],\end{aligned}$$

where the constants have all been determined in Appendix A.

Also, the values of ν_{i_1}, $i_1=1,\ldots,29$, and δ_{j_1}, $j_1=1,\ldots,8$ used in the expression of drag are defined as follows:

$$\begin{aligned}\nu_1 &= 2(\beta_1^2-8)\omega_2,\\ \nu_2 &= 4(\beta_1^2+4)\omega_2,\\ \nu_3 &= (\beta_1^2-\alpha_1^2-\alpha_1-9)^2,\\ \nu_4 &= \sqrt{\nu_3}(2\beta_1^2+\alpha_1^2+\alpha_1+9),\\ \nu_5 &= \sqrt{\nu_3}\eta_1^3+2\beta_1^2+\alpha_1^2+\alpha_1+9,\\ \nu_6 &= (\alpha_1+3)\beta_1^2-\omega_6,\\ \nu_7 &= \omega_6+2(\alpha_1+3)\beta_1^2,\\ \nu_8 &= \beta_1^2\omega_5+2\alpha_1^5+8\alpha_1^4+60\alpha_1^3+126\alpha_1^2+360\alpha_1+324,\\ \nu_9 &= 3\alpha_1^4+14\alpha_1^3+3(27\alpha_1^2+46\alpha_1+23),\end{aligned}$$

$$
\begin{aligned}
\nu_{10} &= 3\alpha_1^4 + 14\alpha_1^3 + 3(19\alpha_1^2 + 30\alpha_1 + 15),\\
\nu_{11} &= 24(\alpha_1 + 1)^2,\\
\nu_{12} &= 30\alpha_1^4 + 121\alpha_1^3 + 120(2\alpha_1^2 + 2\alpha_1 + 1),\\
\nu_{13} &= 3\beta_1^4\omega_3 - \beta_1^2\nu_9 + 8\nu_{10},\\
\nu_{14} &= -4\beta_1^2\nu_{12} + \beta_1^4\nu_{11} - 32\nu_{10},\\
\nu_{15} &= (\alpha_1 + 1)\omega_2,\\
\nu_{16} &= 3\alpha_1^5 + 16\alpha_1^4 + 114\alpha_1^3 + 345\alpha_1^2 + 468\alpha_1 + 234,\\
\nu_{17} &= 60\alpha_1^5 + 301\alpha_1^4 + 1254\alpha_1^3,\\
\nu_{18} &= 2397\alpha_1^2 + 2520\alpha_1 + 1260,\\
\nu_{19} &= (\alpha_1 + 1)\omega_{12},\\
\nu_{20} &= \alpha_1^6 + 6\alpha_1^5 + 41\alpha_1^4 + 72\alpha_1^3 + 12\alpha_1^2 - 72\alpha_1 - 36,\\
\nu_{21} &= 5\alpha_1^6 + 30\alpha_1^5 + 167\alpha_1^4 + 474\alpha_1^3 + 858\alpha_1^2 + 1008\alpha_1 + 504,\\
\nu_{22} &= 48\omega_{11} - 4\beta_1^2\nu_{16} + 12\beta_1^4\nu_{15},\\
\nu_{23} &= -96\omega_{11} - 4\beta_1^2(\nu_{18} + \nu_{17}) + 48\beta_1^4\nu_{15},\\
\nu_{24} &= \beta_1^4\nu_{19} - \beta_1^2\nu_{20},\\
\nu_{25} &= 24(\beta_1^4\nu_{19} - \beta_1^2\nu_{21}),\\
\nu_{26} &= 5\omega_1^2 + 20\beta_1^2\omega_1 + 10\eta_1^3\nu_4 + 5\eta_1^6\nu_3 + 20\beta_1^4,\\
\nu_{27} &= 10(\omega_1\omega_6 - \beta_1^2\omega_5 + (\alpha_1 + 3)\beta_1^4),\\
\nu_{28} &= 5\omega_6^2 - 10(\alpha_1 + 3)\beta_1^2\omega_6 + 5(\alpha_1 + 3)^2\beta_1^4,\\
\nu_{29} &= 10(2\beta_1^4\omega_7 - \omega_6^2 - (\alpha_1 + 3)\beta_1^2\omega_6),\\
\delta_1 &= \nu_2 + \eta_1^3\nu_1,\\
\delta_2 &= 2\Delta_3(\beta_1^2\eta_1^3 + 2\beta_1^2),\\
\delta_3 &= 4\beta_1^2\omega_8 + \eta_1^3\nu_{14} + 2\eta_1^6\nu_{13} + \beta_1^4\nu_{11} + 16\nu_{10},\\
\delta_4 &= 48\omega_{11} + 8\beta_1^2\omega_{10} + \eta_1^3\nu_{23} + \eta_1^6\nu_{22} + 48\beta_1^4\nu_{15},\\
\delta_5 &= 12\beta_1^2\omega_{13} + \eta_1^3\nu_{25} + 6\eta_1^6\nu_{24} + 24\beta_1^4\nu_{19},\\
\delta_6 &= \omega_{14} + \eta_1^3(40(\alpha_1 + 3)\beta_1^4 - 10\nu_8) + \eta_1^6\nu_{27},\\
\delta_7 &= \omega_{15} + \eta_1^3\nu_{29} + \eta_1^6\nu_{28},\\
\delta_8 &= \nu_{26}\chi_1^2.
\end{aligned}
$$

Conflicts of interest

Authors declare that they have no conficts of interest.

References

1. M. Gholinia, M.E. Hoseini, S. Gholinia, *A numerical investigation of free convection MHD flow of Walters-B nanofluid over an inclined stretching sheet under the impact of Joule heating*, Thermal Science and Engineering Progress, **11**, 272–282, 2019.
2. Roberts, Paul Harry, *An Introduction to Magnetohydrodynamics*, **6**, Longmans, London, 1967.
3. H.P.G. Darcy, *Les Fontaines Publiques de la Ville de Dijon*, Victor Delmont, Paris, 1856.
4. H.C. Brinkman, *Calculation of viscous force exerted by flowing fluid on dense swarm of particles*, Applied Science Research, **A**, 27–34, 1947.
5. G.S. Beavers, D.D. Joseph, *Boundary condition at a naturally permeable wall*, Journal of Fluid Mechanics, **30**, 197–207, 1967.
6. P.G. Saffman, *On the boundary condition at the surface of a porous medium*, Studies in Applied Mathematics, **50**, 93–101, 1971.
7. A.I. Leonov, *The slow stationary flow of a viscous fluid about a porous sphere*, Journal of Applied Mathematics and Mechanics, **26**, 564–566, 1962.
8. D.D. Joseph, L.N. Tao, *The effect of permeability on the slow motion of a porous sphere*, Journal of Applied Mathematics and Mechanics, **44**, 361–364, 1964.
9. D.N. Sutherland, C.T. Tan, *Sedimentation of a porous sphere*, Chemical Engineering Science, **25**, 1948–1950, 1970.
10. G. Neale, N. Epstein, *Creeping flow relative to permeable spheres*, Chemical Engineering Science, **28**, 1865–1874, 1973.
11. I.P. Jones, *Low Reynolds number flow past a porous spherical shell*, Mathematical Proceedings of the Cambridge Philosophical Society, **73**, 231–238, 1973.
12. S.K.L. Rao, T.K.V. Iyengar, *The slow stationary flow of incompressible micropolar fluid past a spheroid*, International Journal of Engineering Science, **19**, 189–220, 1981.
13. H. Jacob Masliyah, G. Neale, K. Malysa, T. G. M. Van de ven, *Creeping flow over a composite sphere: solid core with porous shell*, Chemical Engineering Science, **42**, 2, 245–253, 1987.
14. G.P. Raja Sekhar, T. Amaranath, *Stokes flow past a porous sphere with an impermeable core*, Mechanics Research Communications, **23**, 5, 449–460, 1996.
15. Z.G. Feng, E.E. Michaelides, *Motion of a permeable sphere at finite but small Reynolds numbers*, Physics of Fluids, **10**, 6, 1375–1383, 1998.
16. W. Jager, A. Mikelic, *On the interface boundary condition of Beavers, Joseph, and Saffman*, SIAM Journal on Applied Mathematics, **60**, 4, 1111–1127, 2000.
17. P. Vainshtein, M. Shapiro, C. Gutfinger, *Creeping flow past and within a permeable spheroid*, International Journal of Multiphase Flow, **28**, 1945–1963, 2002.
18. A. Bhattacharyya, G.P. Raja Sekhar, *Viscous flow past a porous sphere with an impermeable core: effect of stress jump condition*, Chemical Engineering Science, **59**, 4481–4492, 2004.

19. S. Senchenko, H.J. Keh, *Slipping Stokes flow around a slightly deformed sphere*, Physics of Fluids, **18**, 8, 088104, 2006.

20. A.C. Srivastava, N. Srivastava, *Flow of a viscous fluid at small Reynolds number past a porous sphere with a solid core*, Acta Mechanica, **186**, 161–172, 2006.

21. D. Srinivasacharya, *Flow past a porous approximate spherical shell*, Zeitschrift fur Angewandte Mathematik und Physik, **58**, 646–658, 2007.

22. J.M. Urquiza, D.N. Dri, A. Garon, M.C. Delfour, *Coupling Stokes and Darcy equations*, Applied Numerical Mathematics, **58**, 525–538, 2008.

23. V.M. Shapovalov, *Viscous fluid flow around a semipermeable sphere*, Journal of Applied Mechanics and Technical Physics, **50**, 4, 584–588, 2009.

24. Y. Cao, M. Gunzburger, F. Hua, X. Wang, *Coupled Stokes-Darcy model with Beavers–Joseph interface boundary condition*, Communications in Mathematical Sciences, **8**, 1, 1–25, 2010.

25. E.I. Saad, *Translation and rotation of a porous spheroid in a spheroidal container*, Canadian Journal of Physics, **88**, 689–700, 2010.

26. A.S. Vereshchagin, S.V. Dolgushev, *Low velocity viscous incompressible fluid flow around a hollow porous sphere*, Journal of Applied Mechanics and Technical Physics, **52**, 3, 406–414, 2011.

27. J. Prakash, G.P. Raja Shekar, M. Kohr, *Stokes flow of an assemblage of porous particles: stress jump condition*, Zeitschrift fur angewandte Mathematik und Physik, **62**, 1027–1046, 2011.

28. P.K. Yadav, S. Deo, *Stokes flow past a porous spheroid embedded in another porous medium*, Meccanica, **47**, 6, 1499–1516, 2012.

29. E.I. Saad, *Stokes flow past an assemblage of axisymmetric porous spheroidal particle in cell models*, Journal of Porous Media, **15**, 9, 849–866, 2012.

30. D. Srinivasacharya, M.K. Prasad, *Creeping motion of a porous approximate sphere with an impermeable core in a spherical container*, European Journal of Mechanics B/Fluids, **36**, 104–114, 2012.

31. D. Srinivasacharya, M.K. Prasad, *Axisymmetric creeping flow past a porous approximate sphere with an impermeable core*, The European Physical Journal Plus, **128**, 9, 2013.

32. D. Srinivasacharya, M.K. Prasad, *Axisymmetric motion of a porous approximate sphere in an approximate spherical container*, Archive of Mechanics, **65**, 6, 485–509, 2013.

33. H.H. Sherief, M.S. Faltas, E.I. Saad, *Slip at the surface of an oscillating spheroidal particle in a micropolar fluid*, ANZIAM Journal, **55**(E), E1–E50, 2013.

34. J. Prakash, G.P. Raja Shekar, *Estimation of the dynamic permeability of an assembly of permeable spherical porous particle using cell model*, Journal of Engineering Mathematics, **80**, 63–73, 2013.

35. P.K. Yadav, S. Deo, M.K. Yadav, A. Filippov, *On hydrodynamic permeability of a membrane built up by porous deformed spheroidal particles*, Colloid Journal, **75**, 5, 611–622, 2013.

36. P.C. Chen, *Fluid extraction from porous media by a slender permeable prolate-spheroid*, Extreme Mechanics Letter, **4**, 124–130, 2015.

37. M. Rasoulzadeh, F.J. Kuchuk, *Effective permeability of a porous medium with spherical and spheroidal Vug and fracture inclusion*, Transport in Porous Media, **116**, 313–644, 2017.

38. A. Tiwari, P.K. Yadav, P. Singh, *Stokes flow through assemblage of non-homogeneous porous cylindrical particle using cell model technique*, National Academy Science Letter, **4**, 1, 53–57, 2018.

39. M.K. Prasad, M. Kaur, *Cell models for viscous fluid past a micropolar fluid spheroidal droplet*, Journal of the Brazilian Society of Mechanical Science and Engineering, **40**, 114, 2018.

40. P.K. Yadav, A. Tiwari, P. Singh, *Hydrodynamic permeability of a membrane built up by spheroidal particles covered by porous layer*, Acta Mechanica, **229**, 4, 1869–1892, 2018.

41. S. Khabthani, A. Sellier, F. Feuillebois, *Lubricating motion of a sphere towards a thin porous slab with Saffman slip condition*, Journal of Fluid Mechanics, **867**, 949–968, 2019.

42. M.C. Lai, M.C. Shiue, K.C. Ong, *A simple projection method for the coupled Navier–Stokes and Darcy flows*, Computational Geosciences, **23**, 21–33, 2019.

43. M.K. Prasad, T. Bucha, *Steady viscous flow around a permeable spheroidal particle*, International Journal of Applied and Computational Mathematics, **5**, 109, 2019.

44. M.K. Prasad, *Boundary effects of a nonconcentric semipermeable sphere using Happel and Kuwabara cell models*, Applied and Computational Mechanics, **15**, 2021.

45. K.R Cramer, S.I. Pai, *Magnetofluid Dynamics for Engineers and Applied Physicists*, McGraw-Hill, New York, 1973.

46. P.A. Davidson, *An Introduction to Magnetohydrodynamics*, Cambridge University Press, Cambridge, 2001.

47. S. Globe, *Laminar steady state magnetohydrodynamic flow in an annular channel*, Physics of Fluids, **2**, 404–407, 1959.

48. R.R. Gold, *Magnetohydrodynamic pipe flow, part I*, Journal of Fluid Mechanics, **3**, 505–512, 1962.

49. N. Rudraiah, B.K. Ramaiah, B.M. Raja Shekar, *Hartmann flow over a permeable bed*, International Journal of Engineering Sciences, **13**, 1, 1975.

50. K. Haldar, S.N. Ghosh, *Effect of a magnetic field on blood flow through an indented tube in the presence of erythrocytes*, Indian Journal of Pure and Applied Mathematics, **25**, 345, 1994.

51. H.P. Mazumdar, U.N. Ganguly, S.K. Venkatesan, *Some effect of a magnetic field on the flow of a Newtonian fluid through a circular fluid*, Indian Journal of Pure and Applied Mathematics, **27**, 5, 519–524, 1996.

52. G.E. Geindreau, J.L. Aurialt, *Magnetohydrodynamic flows in porous media*, Journal of Fluid Mechanics, **466**, 343–363, 2002.

53. V.K. Verma, S. Datta, *Magnetohydrodynamic flow in a channel with varying viscosity under transverse magnetic field*, Advance Theory of Applied Mechanics, **3**, 53–66, 2010.

54. D.V. Jayalakshmamma, P.A. Dinesh, M. Sankar, *Analytical study of creeping flow past a composite sphere: solid core with porous shell in presence of magnetic field*, Mapana Journal of Science, **10**, 2, 11–24, 2011.

55. B.G. Srivastava, S. Deo, *Effect of magnetic field on the viscous fluid flow in a channel filled with porous medium of variable permeability*, Applied Mathematics and Computations, **219**, 8959–8964, 2013.

56. B.G. Srivastava, P.K. Yadav, S. Deo, P.K. Singh, A. Filippov, *Hydrodynamic permeability of a membrane composed of porous spherical particles of uniform magnetic field*, Colloid Journal, **76**, 6, 725–738, 2014.

57. V.K. Verma, S.K. Singh, *Magnetohydrodynamic flow in a circular channel filled with a porous medium*, Journal of Porous Media, **18**, 9, 923–928, 2015.

58. P.K. Yadav, S. Deo, S.P. Singh, A. Filippov, *Effect of magnetic field on the hydrodynamic permeability of a membrane built up by porous spherical particles*, Colloid Journal, **79**, 1, 160–171, 2017.

59. E.I. Saad, *Effect of magnetic fields on the motion of porous particles for Happel and Kuwabara models*, Journal of Porous Media, **21**, 7, 637–664, 2018.

60. M.K. Prasad, T. Bucha, *Effect of magnetic field on the steady viscous fluid flow around a semipermeable spherical particle*, International Journal of Applied and Computational Mathematics, **5**, 98, 2019.

61. M.K. Prasad, T. Bucha, *Impact of magnetic field on flow past cylindrical shell using cell model*, Journal of the Brazilian Society of Mechanical Sciences and Engineering, **41**, 320, 2019.

62. M.K. Prasad, T. Bucha, *Creeping flow of fluid sphere contained in a spherical envelope: magnetic effect*, SN Applied Sciences, **1**, 1594, 2019.

63. P.K. Yadav, *Influence of magnetic field on the Stokes flow through porous spheroid: Hydrodynamic permeability of a membrane using cell model technique*, International Journal of Fluid Mechanics Research, **47**, 3, 273–290, 2020.

64. M.K. Prasad, T. Bucha, *Magnetohydrodynamic creeping flow around a weakly permeable spherical particle in cell models*, Pramana Journal of Physics, **94**, 24, 2020.

65. M.K. Prasad, T. Bucha, *MHD viscous flow past a weakly permeable cylinder using Happel and Kuwabara cell models*, Iranian Journal of Science and Technology, Transaction A, Science, **44**, 1063–1073, 2020.

66. M.K. Prasad, T. Bucha, *Effect of magnetic field on the slow motion of a porous spheroid: Brinkman's model*, Archive of Applied Mechanics, **91**, 1, 2021.

67. T. Bucha, M.K. Prasad, *Slow flow past a weakly permeable spheroidal particle in a hypothetical cell*, Archive of Mechanical Engineering, **68**, 2, 27, 2021.

68. M.K. Prasad, M. Kaur, T. Bucha, *Slow motion past a spheroid implanted in a Brinkman medium: Slip condition*, International Journal of Applied and Computational Mathematics, **7**, 162, 2021.

69. P.K. Yadav, S. Jaiswal, J.Y. Puchakatla, *Flow through membrane built up by impermeable spheroid coated with porous layer under the influence of uniform magnetic field: effect of stress jump condition*, European Physics Journal Plus, **136**, 27, 2021.

70. L. DRAGOS, *Magnetofluid Dynamics*, Abacus Press, London, 1975.

71. C. EVCIN, Ö. ÜGUR, M. TEZER-SEZGIN, *Determining the optimal parameters for the MHD flow and heat transfer with variable viscosity and Hall effect*, Computers & Mathematics with Applications, **76**, 6, 1338–1355, 2018.

72. J. HAPPEL, H. BRENNER, *Low Reynolds Number Hydrodynamics*, Englewood Cliffs, Prentice-Hall, NJ, 1965.

73. D.A. NIELD, A. BEJAN, *Convection in porous media*, Studies in Applied Mathematics 3, Springer, New York, 2006.

74. H. RAMKISSOON, *Slip flow past an approximate spheroid*, Acta Mechanica, **123**, 227–233, 1997.

75. K.B. NAKSHATRALA, M.S. JOSHAGHANI, *On interface conditions for flows in coupled free-porous media*, Transport in Porous Media, **130**, 577–609, 2019.

76. A. PROSPERETTI, *Viscous effects on perturbed spherical flows*, Quarterly of Applied Mathematics, **34**, 4, 339–352, 1977.

Received August 03, 2021; revised version November 01, 2021.
Published online 31 December, 2021.